



# CHANS-SD-YRB V1.0: A System Dynamics model of

# the coupled human-natural systems for the Yellow

3	River Basin
4	Shan Sang <sup>1,2</sup> , Yan Li <sup>1,2*</sup> , Shuang Zong <sup>1,2</sup> , Lu Yu <sup>1,2</sup> , Shuai Wang <sup>1,2</sup> , Yanxu Liu <sup>1,2</sup> ,
5	Xutong Wu <sup>1,2</sup> , Shuang Song <sup>1,2</sup> , Wenwu Zhao <sup>1,2</sup> , Xuhui Wang <sup>3</sup> , Bojie Fu <sup>4</sup>
6	<sup>1</sup> State Key Laboratory of Earth Surface Processes and Hazards Risk Governance (ESPHR), Beijing
7	Normal University, Beijing, China
8	<sup>2</sup> Institute of Land Surface System and Sustainable Development, Faculty of Geographical Science,
9	Beijing Normal University, Beijing, China
10	<sup>3</sup> Institute of Carbon Neutrality, Laboratory for Earth Surface Processes, College of Urban and
11	Environmental Sciences, Peking University, Beijing 100871, China
12	<sup>4</sup> State Key Laboratory of Regional and Urban Ecology, Research Center for Eco-Environmental
13	Sciences, Chinese Academy of Sciences, Beijing 100085, China
14	
15	Corresponding Author:
16	Yan Li, Ph.D.
17	Institute of Land Surface System and Sustainable Development, Faculty of Geographical Science,
18	Beijing Normal University, Beijing, 100875, China
19	Email: <u>yanli.geo@gmail.com</u>
20	
21	Abstract: Modeling the coupled human-natural systems (CHANS) is vital for
22	understanding human-natural interactions and achieving regional sustainability,
23	offering a powerful tool to alleviating human-water conflicts, ensuring food security,
24	thereby supporting the region's pathway toward sustainable development. However,
25	the scarcity of regional-scale CHANS models constrains progress in practical
26	applications for regional sustainability. The Yellow River basin (YRB) is an ideal region

1

50

51

52

53

54





27 for modeling regional CHANS due to its closely coupled human and natural systems, 28 which are stressed by water and ecosystem fragility. Here, we developed the CHANS-29 SD-YRB model using the System Dynamics approach, integrating 10 sectors essential 30 for modeling human-water interactions of the basin, including five human sectors 31 (Population, Economy, Energy, Food, and Water Demand) and five natural sectors (Water Supply, Sediment, Land, Carbon, and Climate). The model can simulate 32 33 evolution and feedbacks of the YRB CHANS annually at provincial and sub-basin 34 scales, while conserving hydrological connectivity between sub-basins. The model can 35 accurately reproduce historical CHANS dynamics, achieving strong quantitative agreement with historical data (R > 0.95 for human sectors and R > 0.7 for natural 36 37 sectors), which supports its applicability for scenario analyses and future projections. 38 We applied the model to explore human-natural system dynamics under a future baseline scenario, assuming the continuation of existing policies and climate projection 39 40 under middle of the road scenario (SSP–RCP 2-4.5). The future projections (2021-2100) 41 indicate that achieving sustainable development in the YRB will remain challenging, 42 though economic growth and food security are expected to improve. Emerging issues, 43 such as ecological-human water trade-offs, labor shortages, reduced sediment load, and 44 limited carbon absorption capacity, may hinder regional long-term sustainability. 45 **Keywords:** coupled human-natural systems, regional modeling, system dynamics, 46 the Yellow River Basin 47 1 Introduction

Coupled human and natural systems (CHANS) emphasize the reciprocal feedback and co-evolution between human and natural systems, offering an integrated framework for diagnosing complex problems and guiding sustainable development (Fu and Li, 2016). While global-scale CHANS research has deepened our knowledge of dynamic feedbacks among Earth's spheres and system evolution under climate change, sustainability challenges often manifest at regional scales, where social and ecological dynamics are more intricately intertwined (Liu et al., 2007). Compared to global





materials with other regions and the global system, e.g., water resources and electricity 56 57 transfers (Dobbs et al., 2023; Zhang et al., 2022a) and trade (Ristaino et al., 2021), resulting in pericoupling and telecoupling of different systems (Liu, 2017). Besides, 58 59 regional CHANS are shaped by more immediate and complex human influences and 60 stressors, such as urban expansion (van Vliet, 2019), ecological protection (Xu et al., 61 2017; Yang et al., 2022), and water resource regulation policies (diversion and 62 allocation) (Song et al., 2024), which alter regional CHANS dynamics. Moreover, due 63 to their diverse ecological and socioeconomic resilience, regional CHANS exhibit heterogeneous responses to external weather events and climate change, as evidenced 64 by differing responses in crop yield (Hasegawa et al., 2021) and economic production 65 to extreme heat and warming (Waidelich et al., 2024). By capturing dynamic 66 interactions of interconnected components, CHANS theories and models enable more 67 68 effective policies and interventions that align ecological integrity with socioeconomic 69 progress (Motesharrei et al., 2016; Verburg et al., 2016). As such, advancing CHANS 70 research is essential for informing adaptive strategies in the face of regional growing 71 environmental and societal pressures. 72 Modeling of CHANS is a frontier area of geographical science and has become a 73 key approach in resources, environment, and climate research. CHANS models serve 74 as essential tools for analyzing the complex dynamics of human-natural interactions 75 and guiding pathways toward sustainability. Numerous modeling approaches have been developed to simulate human-natural interactions at global scale, including system 76 77 dynamics (SD) models (e.g., ANEMI (Breach and Simonovic, 2021), FeliX (Rydzak et 78 al., 2013; Ye et al., 2024), and FRIDA (Rajah et al., 2025)), integrated assessment 79 models (IAMs) (Vaidyanathan, 2021), integrated Earth system model (iESM) (Jain et 80 al., 2022) and synchronously coupled human component in the earth system model 81 (E3SM-GCAM) (Di Vittorio et al., 2025). These models effectively characterize 82 human-natural interactions at the global scale, and have been applied to assess the 3

CHANS, regional CHANS are open systems that continuously exchange energy and





economic damage (Wang et al., 2020b), fatalities increase and welfare loss (Dottori et 84 85 al., 2018)), and humans' feedback on the Earth system, such as those from climate mitigation on water and food security (Cheng et al., 2022; Fujimori et al., 2022). 86 87 However, global models cannot represent the complex dynamics of human-natural 88 interactions at the regional level, due to the openness of regional CHANS (Verburg et 89 al., 2016), diversified regional human and natural processes (Clark et al., 2015), with 90 locally heterogeneous responses to disturbances (Baldos et al., 2023). Moreover, the 91 coarse spatiotemporal resolution of global models limits their capacity to support effective decision-making for regional development (X. Li et al., 2018). 92 93 To address this limitation, many regional CHANS models have been developed at 94 various regional scales (e.g., national, basin, and urban) using System Dynamics (SD) and agent-based modeling (ABMs) techniques. Notable examples include the ANIME-95 96 Yangtze model (Jiang et al., 2022), the T21-China (Qu et al., 2020), and the iSDG-97 Australia model (Allen et al., 2019), all based on SD, the Jordan Water Model (Yoon et al., 2021) based on ABM, as well as integrated models in the San Juan River Basin 98 99 (Hyun et al., 2019) and the Heihe River Basin (Li et al., 2021). These models are 100 designed to capture finer-scale dynamics and region-specific human-natural 101 interactions, since they embed localized characteristics (e.g., fishing ban, reservoir 102 operation strategies, demographic policies, transboundary flows) and account for 103 heterogeneity overlooked by global models. As a result, regional CHANS models offer 104 stronger policy relevance, providing actionable insights for national, basin, and urban 105 decision-making, and advancing CHANS research across multiple scales. 106 The Yellow River Basin (YRB) in China is one of the regions where conflicts 107 between human and natural systems are most acute and complex, particularly in terms 108 of human-water relations, due to the severe imbalance between socioeconomic 109 development and natural hydrological, ecosystem processes. The YRB faces severe 110 water stress, with the water resource utilization rate exceeding 80% (Feng and Zhu,

impacts of climate change on human society (e.g., agriculture (Monier et al., 2018),

112

113

114

115

116 117

118

119

120121

122

123124

125

126

127

128

129

130

131

132133

134

135

136

137

138





2022; Zhang et al., 2022b). Intensive water extraction has triggered a series of ecological and environmental issues, including flow interruptions, water pollution, and declining groundwater levels, all of which in turn constrain socioeconomic development. The Yellow River traverses the Loess Plateau (Zhu et al., 2019), where severe soil erosion makes the Yellow River one of the most sediment-laden rivers globally (Fu et al., 2011; Yin et al., 2021). The pronounced spatial and temporal variability in streamflow and sediment load leads to significant riverbed aggradation, frequent flooding, and disruption of agricultural production and other livelihood activities (Miao et al., 2016). Due to internal hydrological connectivity, sub-basins are highly interconnected and are susceptible to upstream influences. Upstream water overuse diminishes downstream availability (Wei et al., 2023), a factor that played a major role in flow interruptions during the 1990s (Changming and Shifeng, 2002; Wang et al., 2019). Ecological challenges differ across the subbasin, with the upstream facing ecosystem degradation and limited water retention (Ning et al., 2022), the midstream characterized by soil erosion and large-scale ecological restoration (Fu et al., 2011), and the downstream focusing on wetland conservation (Fu et al., 2023). Policy measures aimed at ecological restoration, such as afforestation and cropland conversion, have increased vegetation cover, reduced sediment loads but also decreased runoff, exacerbating water scarcity (Feng et al., 2016; Wang et al., 2016). These interlinked dynamics underscore the YRB as a complex coupled human-natural system, where addressing environmental challenges requires an integrated, systems-oriented approach. The existing models for the YRB are typically designed for specific problems with a narrow application focus and only represent a limited set of human and natural components within the CHANS. These include limited nature-to-human impact pathways, e.g., low flows threatening farmers' livelihoods (Liu et al., 2008), the damage of floods and droughts on agriculture (Zhang et al., 2015), as well as human-to-nature impact pathways, e.g., effects of ecological restoration policy on hydropower and water-sediment-carbon dynamics (Wu et al., 2025; Yan et al., 2024), and the impacts

https://doi.org/10.5194/egusphere-2025-5597 Preprint. Discussion started: 19 November 2025 © Author(s) 2025. CC BY 4.0 License.





139 of irrigation water-saving and salinity-control practices on crop yield and water productivity (Wu et al., 2023). These models focus on isolated components of CHANS, 140 141 with limited consideration of fully coupled human-natural interactions, which limits 142 their capacity to represent full human-natural interactions and support regional 143 decision-making. To address the gap in CHANS modeling for the YRB, following our previously 144 145 proposed CHANS modeling framework for the basin (Sang et al., 2025), we 146 implemented the framework to develop the coupled human and natural systems model 147 for the YRB (CHANS-SD-YRB) using the System Dynamics approach. Through 148 dynamic interaction with policies, climate change, human activities, and environmental 149 feedbacks, the CHANS-SD-YRB model provides a platform for predicting system dynamics, conducting scenario analyses, evaluating policies, and optimizing water-150 food-carbon synergies. This study offers both theoretical and practical insights for 151 152 advancing regional CHANS modeling and promoting sustainable development in the 153 YRB.



# 154 2 Description of the CHANS-SD-YRB

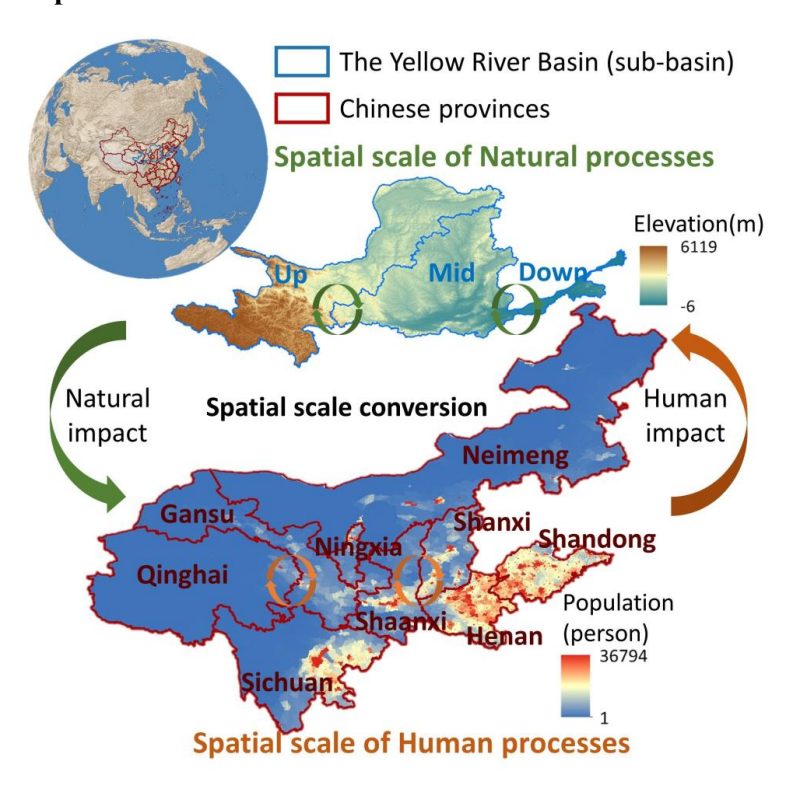


Fig.1 Geolocation of the Yellow River Basin and boundary of the natural and human processes in the CHANS-SD-YRB model. Natural processes are simulated at the subbasin scale (base map: elevation), and human processes at the provincial scale across nine provinces (base map: population density in 2020).

We developed the CHANS-SD-YRB based on system dynamics, a method well-suited for capturing complex system behaviors characterized by nonlinearity, multi-level structures, and feedback loops (Akhtar et al., 2013). The model was constructed and implemented using the VENSIM DSS (Ventana Systems, 2023) software platform, operating on an annual time step. The CHANS-SD-YRB simulates both human and natural processes for historical simulations (1981–2020) and future projections (2021–2100). Human processes are simulated at the provincial scale, covering the nine provinces along the Yellow River (Qinghai, Sichuan, Gansu, Ningxia, Neimeng,





Shaanxi, Shanxi, Henan, and Shandong), while natural processes are simulated at the sub-basin scale (up-, mid-, and downstream) (Fig.1). The model is designed to capture the various interactions within and between different components of human system and natural system across administrative and hydrological units. The spatial scale conversion between provincial and sub-basin levels relies on weights (e.g., the proportion of sub-basin-level values to provincial total values) derived from historical high-resolution gridded datasets of human-related variables. These weights enable disaggregation of provincial outputs to the sub-basin level (see Supporting Information S4 for details). Given the availability of gridded data for human processes and the strong correlations among relevant variables, gridded population and GDP data were used as proxies to disaggregate provincial-level outputs to the sub-basin scale (Table S3).

#### 2.1 Model structure

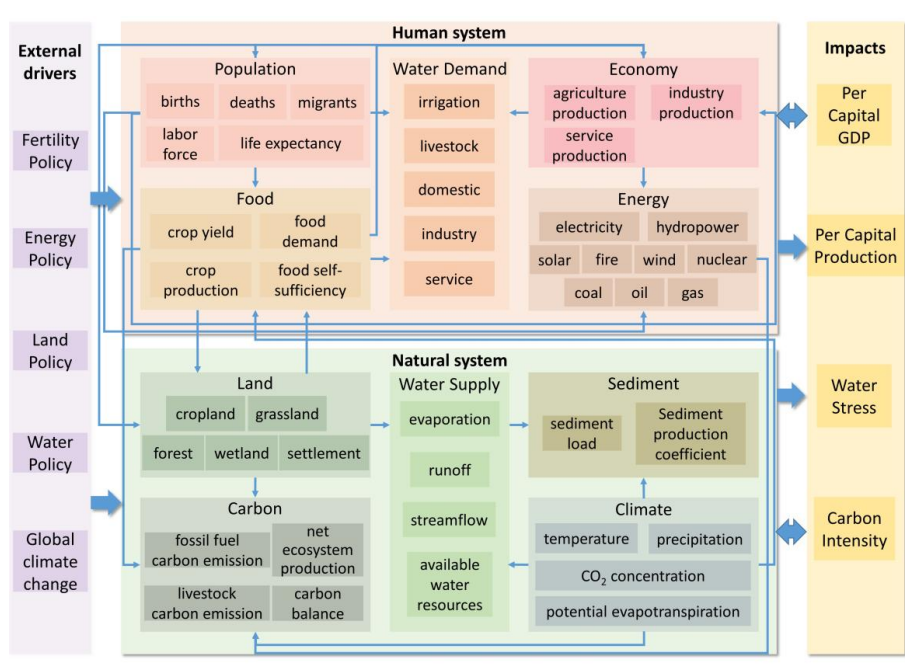


Fig.2 Structure of the CHANS-SD-YRB, which shows sectors of human and natural systems, their key processes and interactions.





184 Drawing on the modeling framework of CHANS in the YRB (Sang et al., 2025), 185 we designed the CHANS-SD-YRB structure (Fig. 2), including five sectors related to 186 human society (Population, Economy, Energy, Food, and Water Demand), and five 187 sectors related to natural ecosystem (Water Supply, Sediment, Land, Carbon, and 188 Climate). 189 These sectors are interconnected to represent various human-natural interactions 190 as summarized below. Key interactions among human system modules are summarized 191 below. The *Population* sector affects food demand (*Food*), residential water use (*Water* 192 Demand), household electricity and gas consumption (Energy), and settlement land area (Land). The sector also interacts dynamically with the Economy sector, where economic 193 194 output influences deaths and migrants, while the labor force, in turn, drives economic 195 production. The *Economy* sector drives energy uses (electricity, coal, oil, and gas use) from Energy, as well as industrial and service water withdrawal from Water Demand. 196 197 The gross agricultural production in the Economy is made up of crop and livestock production (Food). The Energy sector produces fossil fuel emissions in the Carbon 198 199 sector. The Food sector is affected by the Land and Climate sector, and it also 200 determines irrigation water withdrawal (Water Demand) and livestock-related 201 emissions (Carbon). Additionally, the Food sector interacts closely with the Land sector, 202 where crop production depends on cropland area, which, in turn, is influenced by food 203 self-sufficiency. The Water Demand sector affects streamflow in the Water Supply 204 sector through consumptive water use. 205 The key interactions among natural system modules are listed below. The Land 206 sector influences evapotranspiration in the Water Supply sector through vegetation 207 coverage, and it influences carbon absorption in Carbon sector through land use area. 208 The carbon absorption is also affected by climatic variables including temperature, 209 precipitation, and CO<sub>2</sub> concentration. Similarly, runoff in the Water Supply sector is 210 affected by precipitation, precipitation intensity (mm/h, the rate of rainfall within one 211 hour calculated from daily data), and potential evapotranspiration. Streamflow





influences sediment dynamics in the Sediment sector together with the Climate sector. 213 In addition, the CHANS dynamics in the YRB are modulated by external drivers, 214 including policies and global climate change that affect various modeled processes (e.g., 215 fertility, energy, land use, and water). With comprehensive representation of CHANS 216 processes and their interactions, the CHANS-SD-YRB model is capable of generating 217 integrated indicators to assess the state of the coupled system, such as per capita GDP, 218 per capita food production, water stress, and carbon intensity. These indicators not only 219 serve as evaluation metrics but also feed back to influence the internal dynamics of the 220 human-natural system in the YRB. 221 2.2 Sector description 222 The CHANS-SD-YRB model focuses on the essential human–natural processes in 223 the YRB, with a particular emphasis on human-water interactions. To this end, it has a comprehensive representation of the full range of natural and human processes that 224 225 influence water use and supply. Formulation of each sector aims to explicitly account for cross-sectoral interactions as fully as possible while remaining sufficiently simple 226 to be implemented within the SD software. Considering data availability and the spatial 227 228 scales of process, human sectors (Population, Economy, Energy, Food, and Water 229 Demand) are simulated at the provincial level, while natural sectors (Water Supply, 230 Sediment, Land, Carbon, and Climate) are simulated at the sub-basin level within the 231 YRB. Next, we describe each sector and its key formulation and provide full details in 232 Supporting Information S2.





## 2.2.1 Population

233

234235

236237

238239

240

241

242

243244

249

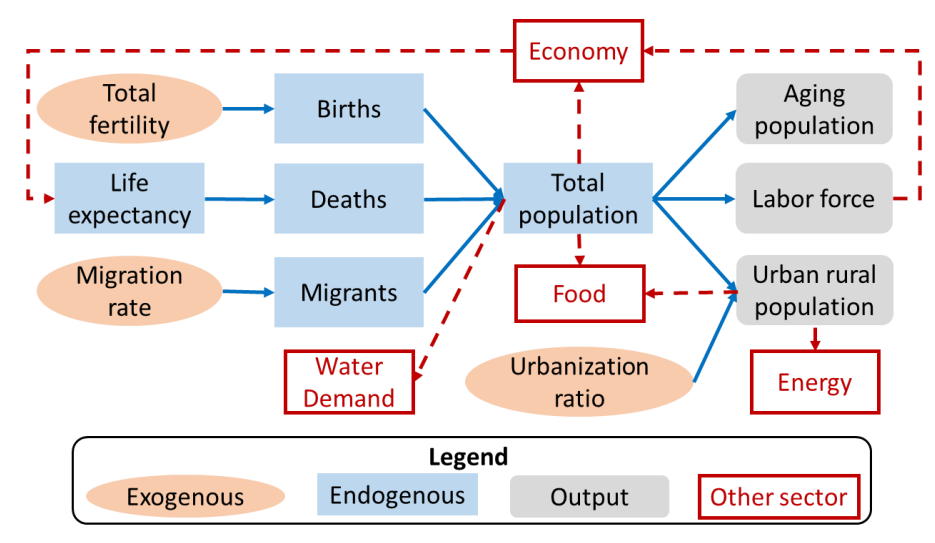


Fig.3 Structure of the *Population* sector. Blue lines indicate connections inside the sector, red dotted lines indicate connections with other sectors.

Population dynamics are represented by birth, death, and migrants, which are determined by a series of social and economic factors. The total population is characterized by age and gender with exogenous urbanization ratios. The output of *Population* sector drives *Economy*, *Energy*, *Food*, and *Water Demand* sectors through labor force, urban and rural populations.

The key variable, total population, is modeled using the age-structured mathematical method (Kemei et al., 2024), which categorizes individuals by one-year age group and gender (Equation 1),

245 
$$Pop_{g,a} = IniPop_{g,a} + \begin{cases} \int (B_{g,a} + NM_{g,a} - D_{g,a})dt, & a = 0 \\ \int (Pop_{g,a} + NM_{g,a} - D_{g,a})dt, & 1 \le a \le 99, a = 100 \text{ and over} \end{cases}$$
246 (1)

247 where *Pop* is population, subscript g and a are gender (g = M is male, g = F is female)

248 and age (a = 0-100 and over);  $IniPop_{g,a}$  is the population in the initial year,  $B_{g,a}$  is the

births (Equation S2),  $D_{g,a}$  is the deaths (Equations S3-S6), and  $NM_{g,a}$  is the net migrants

250 (i.e., immigrants – emigrations, Equations S7-S8).





### 2.2.2 Economy

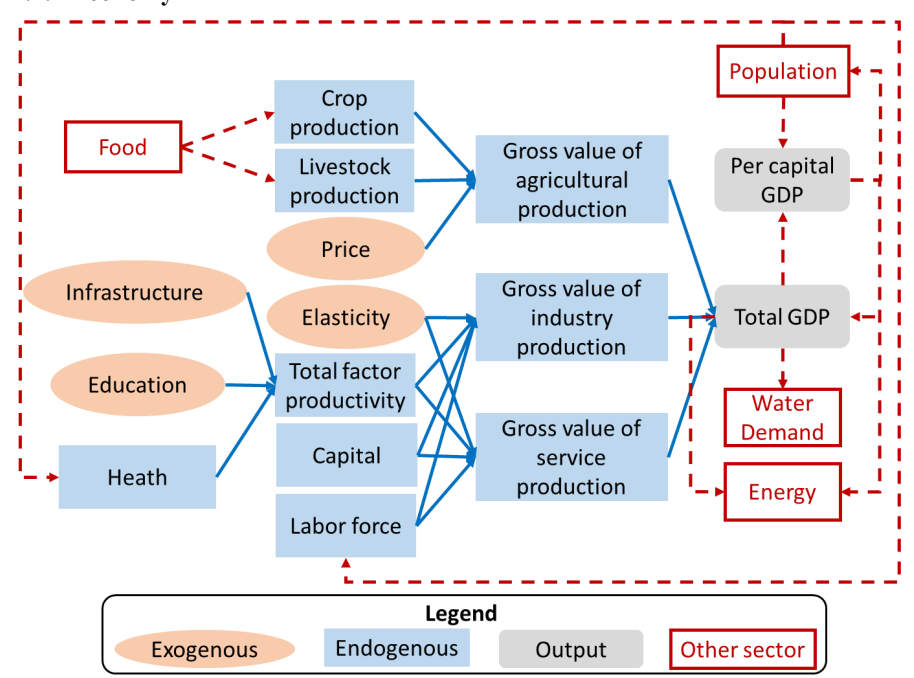


Fig.4 Structure of the *Economy* sector. Blue lines indicate connections inside the sector, red dotted lines indicate connections with other sectors.

The *Economy* sector simulates production activities in agriculture, industry, and services, which in turn drive changes in the *Population*, *Energy*, and *Water Demand* sectors.

The gross product of industry and services is calculated using the Cobb-Douglas production function (Cobb and Douglas, 1928) to account for multiple factors in the economy (Equation 2). Exogenous variables (infrastructure, education, and elasticity), and endogenous variables (health and labor force) from the *Population* sector (Equations S10-S17) all affect the gross domestic product in industry and service ( $GDP_s$ ),

$$GDP_{s} = IniGDP_{s} \times TFP_{s} \times \left(\frac{L_{s}}{IniL_{s}}\right)^{1-\alpha_{s}} \times \left(\frac{K_{s}}{IniK_{s}}\right)^{\alpha_{s}}$$
 (2)

where subscript s represents industry and service,  $IniGDP_s$  is the initial GDP;  $TFP_s$  is the total factor productivity;  $L_s$  represents the labor force and  $IniL_s$  is its initial value





(from *Population* sector);  $\alpha_s$  is capital and I- $\alpha_s$  is labor elasticities, from T21-China (Qu et al., 2020);  $K_s$  and  $IniK_s$  refer to the capital stock and its initial level.

Gross agricultural production includes crop and livestock production from *Food* sector, calculated by their respective prices (Equations S18-S19).

### 2.2.3 Energy

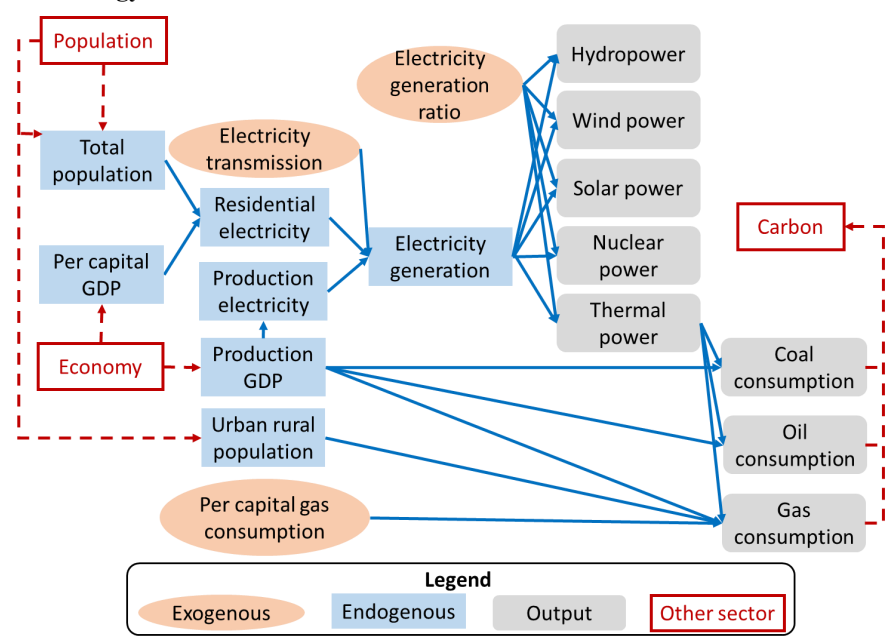


Fig.5 Structure of the *Energy* sector. Blue lines indicate connections inside the sector, red dotted lines indicate connections with other sectors.

The *Energy* sector simulates production, consumption, and the structure of energy, encompassing coal, oil, gas, and electricity. Coal, oil, and gas consumption are derived from linear relationships between historical sectoral GDP and corresponding consumption (Equations S22-S24). Electricity generation is divided into residential and industrial uses, the former is estimated from the linear fit of historical per capita GDP and residential demand, and the latter is calculated using electricity intensity data from the China Energy Statistical Yearbook (NBSC, 2020a) (Equations S20-S21). Crossprovincial electricity transmission is also incorporated according to the same yearbook. The shares of electricity generated from thermal, hydro, wind, solar, and nuclear





sources are determined by exogenously specified ratios, as reported in the China Energy
Statistical Yearbook (NBSC, 2020a). Fossil fuel consumption drives carbon emissions
in the *Carbon* sector.

#### 2.2.4 Food

287

288

289290

291

292

293

294

295

296

297

298

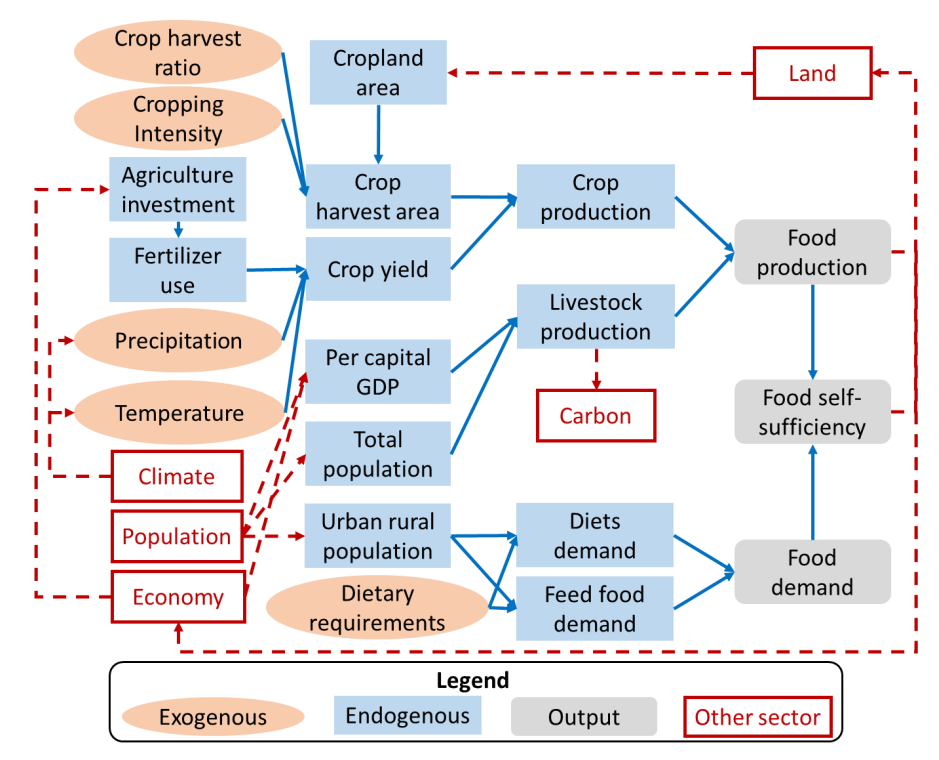


Fig.6 Structure of the *Food* sector. Blue lines indicate connections inside the sector,

red dotted lines indicate connections with other sectors.

The Food sector simulates the production of livestock and crops, and food demand, and these productions directly affect gross agricultural production in the Economy sector. Livestock production ( $Livestock_{pro}$ ) is calculated by an empirical function, driven by economic development and population growth (Equation 3),

$$Livestock_{pro} = Pop \times \left(Para_{GL1} + (Para_{GL2} - Para_{GL1}) \times \frac{PC_{GDP}}{PC_{GDP} + Const_{GL}}\right)$$
(3)

where  $Para_{GL1}$ ,  $Para_{GL2}$  and  $Const_{GL}$  are parameters obtained by fitting the historical per capita meat production and per capita GDP ( $PC_{GDP}$ ) data.

Crop production ( $Crop_{pro}$ ) is determined by the yield ( $Yield_c$ ) and harvest area ( $PA_c$ )





of seven major crop types (subscript c): rice, wheat, corn, soybeans, cotton, potatoes, and oil crops (Equation 4). The harvest area is influenced by cropland area from the *Land* sector, exogenous cropping intensity and crop harvest ratio. Crop yields are positively affected by agricultural investment from the *Economy* sector, along with effects of precipitation, temperature, and  $CO_2$  concentration from the *Climate* sector (Equations S26-S31).

$$Crop_{pro} = \sum_{c=1}^{7} Yield_c \times PA_c \tag{4}$$

Food demand encompasses both staple and feed grain demand, which are determined by population size from *Population* sector and dietary patterns (Equations S33-S36).

### 2.2.5 Water Demand

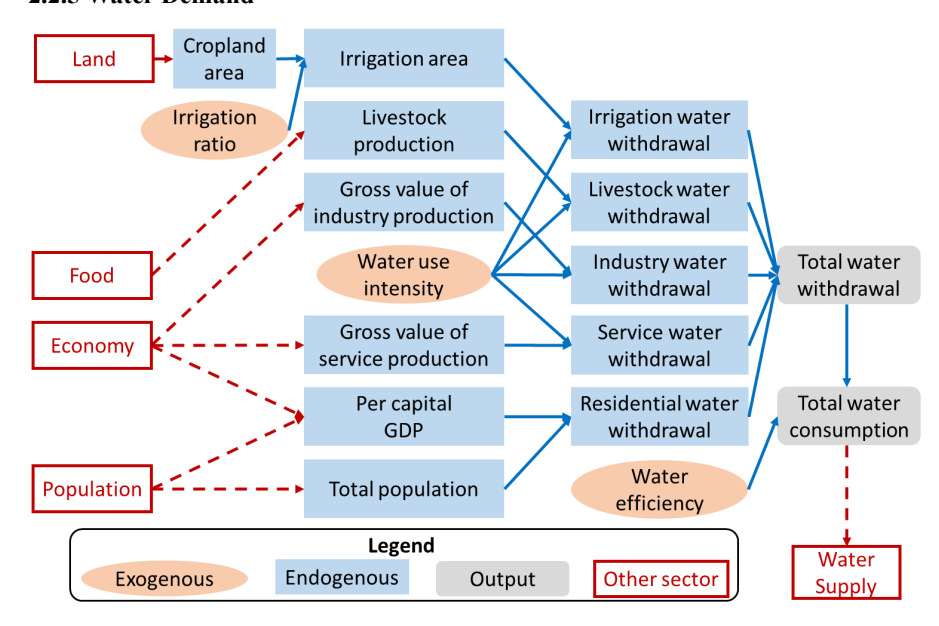


Fig.7 Structure of the *Water Demand* sector. Blue lines indicate connections inside the sector, red dotted lines indicate connections with other sectors.

The *Water Demand* sector simulates water withdrawal (*WW*) and consumption (*WC*) across multiple uses—irrigation, livestock, industry, services, and residential—in the nine provinces of the YRB. Water consumption is derived as the product of water





- withdrawal and water use efficiency reported in the Water Resources Bulletin (YRCCMWR, 2020) (Equations S37-S38), which affects the *Water Supply* sector.
- Irrigation water withdrawal (*WWirr*) is estimated based on exogenous irrigation water use intensity (*WWIirr*), and irrigation cropland ratios (*IR*) from the China Agricultural Yearbook (MAARA, 2020), and cropland area (*Areacropland*) provided by the *Land* sector (Equation 5).

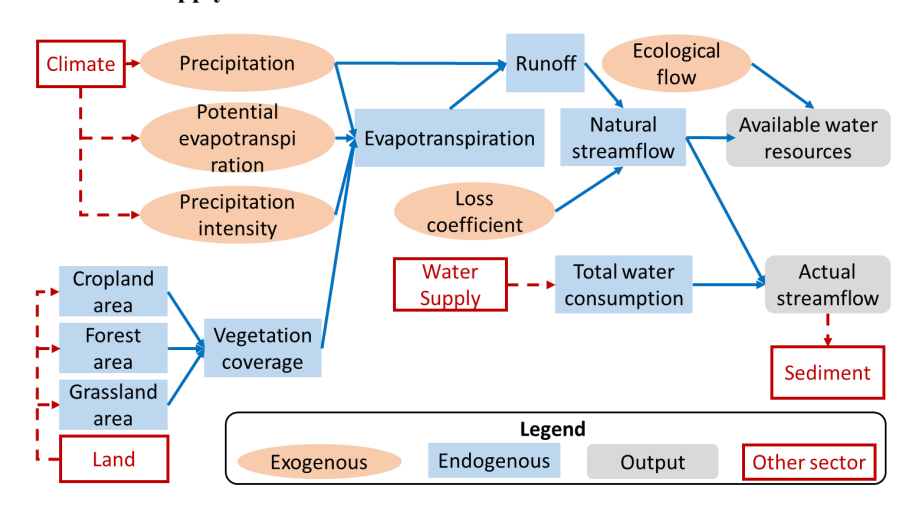
$$WW_{irr} = WWI_{irr} \times Area_{Cropland} \times IR$$
 (5)

- The water withdrawal for livestock, industry, and services is also driven by exogenous sectoral water use intensities collected from the China Statistical Yearbook and National Long-term Water Use Dataset of China (Zhou et al., 2020), in combination with livestock production from the *Food* sector, economic output from the *Economy* sector (Equations S40-S43).
- Residential water withdrawal ( $WW_{res}$ ) is obtained from the empirical function, driven by economic development and population growth (Equation 6),

330 
$$WW_{res} = Pop \times \left(Para_{GD1} + (Para_{GD2} - Para_{GD1}) \times \frac{PC_{GDP}}{PC_{GDP} + Const_{GD}}\right)$$
 (6)

where  $Para_{GD1}$ ,  $Para_{GD2}$ , and  $Const_{GD}$  are parameters obtained by fitting the historical per capita domestic water use with per capita GDP ( $PC_{GDP}$ ).

## 2.2.6 Water Supply



333





335 Fig.8 Structure of the Water Supply sector. Blue lines indicate connections inside the 336 sector, red dotted lines indicate connections with other sectors. 337 The Water Supply sector simulates runoff, discharge, and their changes in each sub-basin. Runoff (R) is determined by precipitation (Pre) and evapotranspiration (ET)338 339 based on the water balance principle derived from the Budyko equation, which is 340 suitable for non-humid regions of China (Yang et al., 2009) (Equation 7). 341 (7) R = Pre - ET342 The ET is calculated by various exogenous climate variables from the Climate sector, and vegetation coverage from the Land sector (Equations 8-9, S46-S48), 343  $ET = \frac{PET \times Pre}{(Pre^n + EP^n)^{\frac{1}{n}}}$ 344 (8)  $n = Para_{E1} \times \left(\frac{\kappa s}{PI}\right)^{Para_{E2}} \times FVC^{Para_{E3}} \times e^{Para_{E4}tan\beta}$ 345 (9)where *PET* is potential evapotranspiration at sub-basin, from the *Climate* sector; *n* is a 346 347 parameter reflecting the basin landscape characteristics, related to saturated hydraulic 348 conductivity (Ks), precipitation intensity (PI), average slope  $(\beta)$ , and fraction of 349 vegetation coverage (FVC); Parael, Parael, Parael, and Parael are parameters fitted 350 from historical data. 351 Runoff and the loss coefficient (defined by the ratio of natural streamflow to runoff) 352 determine the natural streamflow due to the water loss during the confluence process 353 (Equation S49). Natural streamflow and ecological flow constraints define the upper 354 limit of available water resources. By integrating human water consumption from the Water Demand sector across sub-basins, the model calculates the actual streamflow 355 356 (Equations S50-S52). Actual streamflow is transferred through hydrological 357 connectivity from upstream to midstream and then to downstream, ultimately reaching 358 the sea, which governs sediment transport processes within the Sediment sector.

### 2.2.7 Sediment

359

360

361

The *Sediment* sector estimates sediment load (*Sed*) for each sub-basin using an empirical model in the literature (Yin et al., 2023b), which links actual streamflow from





362 the Water Supply sector to sediment transport,

$$Sed = Para_{SS} \times AS + Const_{SS}$$
 (10)

364 where Parass and Constss are derived from linear fitting of historical hydrological

365 station data on actual streamflow and sediment load.

### 2.2.8 Land

366

367

368

370

371

372

373

374

375

376

377

378

379

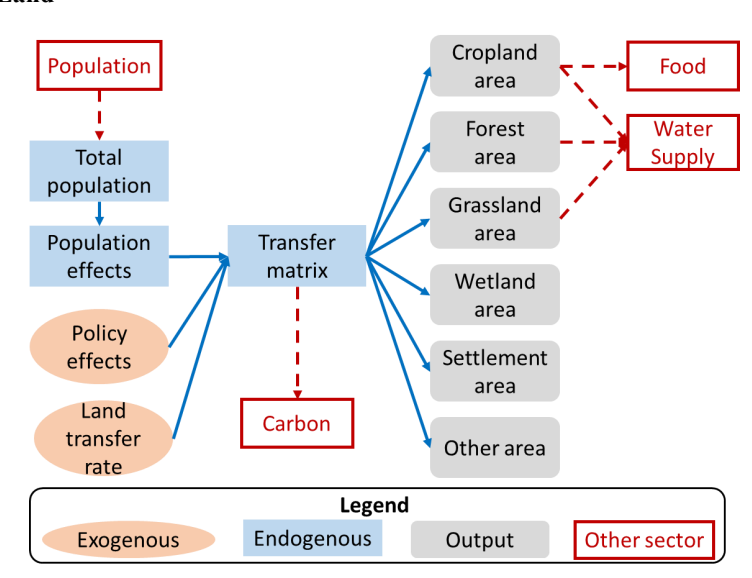


Fig.9 Structure of the Land sector. Blue lines indicate connections inside the sector,

red dotted lines indicate connections with other sectors.

The Land sector simulates the area changes of six land use types (cropland, forest, grassland, wetland, settlement, and others) based on the land transfer matrix obtained from historical remote sensing data (Xu et al., 2018). The land transfer matrix calculates the inflow and outflow of each land category and can be configured to represent the influence of future land use drivers. This sector outputs vegetation area (including forest, grassland, and cropland), which influences the Water Supply sector. Cropland area changes impact the Food sector, while land use conversion also plays a role in the Carbon sector.

Based on the initial land use area ( $IniArea_i$ ), the transfer matrix determines the area ( $Area_i$ ) allocated to each land use type (Equations 11, S55-S61),





380 
$$Area_i = IniArea_i + \int \left(\sum_{i=1}^6 FTM_{i,j} - \sum_{j=1}^6 FTM_{i,j}\right) dt \tag{11}$$

where  $FTM_{i,j}$  is the finial land use transfer matrix, indicating the area of land use i

transferred to land use j, i and j represent six land use type.

#### 2.2.9 Carbon

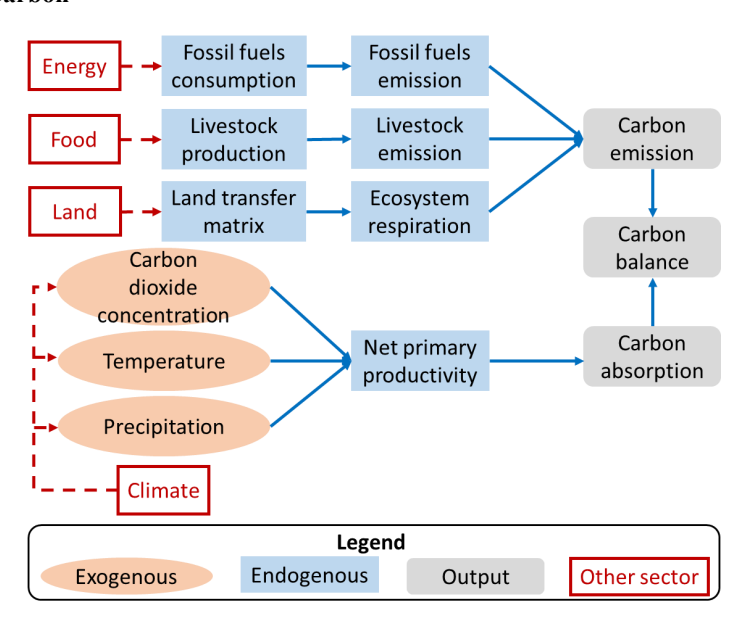


Fig.10 Structure of the *Carbon* sector. Blue lines indicate connections inside the sector, red dotted lines indicate connections with other sectors.

The *Carbon* sector simulates the basin's carbon balance processes, including carbon emission and absorption, adapted from the carbon cycle of ANEMI (Davies and Simonovic, 2011). Carbon emissions (*CE*) encompass fossil fuel emissions, and livestock emission, and ecosystem respiration, which are influenced by outputs from the *Energy, Food*, and *Land* sectors.

Fossil fuel and livestock emissions are calculated based on fossil fuel consumption, livestock production, and their respective emission coefficients. Ecosystem emissions include carbon released from burning as well as from the decomposition of biomass, litter, humus, and charcoal, which are determined by carbon pools' lifespans, decomposition factor, and respiration coefficients (Equations S64-S88).





397	Carbon absorption (CA) is determined by net primary productivity (NPP) and land
398	use area. NPP is influenced by climate factors, including CO2 concentration,
399	temperature, and precipitation (Equations 12, S63),
400	$CA = \sum_{i=1}^{6} NPP_i \times Area_i \tag{12}$
401	where i represent land use type, land use area (Areai) from the Land sector.
402	2.2.10 Climate
403	The Climate sector supplies both historical and projected climate data essential for
404	the Water Supply, Food, and Carbon sectors. The key climate variables comprise
405	temperature and precipitation (at the sub-basin and provincial levels), as well as
406	potential evapotranspiration, precipitation intensity, and CO2 concentration (at the sub-
407	basin level). These variables are treated as exogenous inputs, without accounting for
408	potential feedbacks from human activities or natural system responses on regional
409	climate patterns.
410	2.3 Data sources
411	In the model, there are more than 100 exogenous variables, some of which are
412	initial variables that drive the simulation. These exogenous variables are derived either
413	from historical statistical data or from fitted results based on historical data (Table S2).
414	All data sources required for the model simulation are listed in Table 1.
415	Table 1. Summary of data sources for the YRB model. Updated from Sang et al.

China Population Census Yearbook (NBSC, 2020b)  China Agricultural Yearbook (MAARA,  Provincial,  1981–	Sector	Variables*	Data sources	Spatial and temporal scale	Time range
Economy GDP, investment, Yearbook (MAARA, • provincial, • 1981–	Population	population, births,	Yearbook (NBSC, 2020c), • China Population Census	1 /	• 1981–2023
China Statistical	Economy	GDP, investment, employment	Yearbook (MAARA, 2020),	*	• 1981–2023

(2025).





Yearbook (NBSC, 20		Yearbook (NBSC, 2020c)				
Energy	Energy electricity, coal, oil, gas consumption • China Energy Statistical Yearbook (NBSC, 2020a)		•	provincial, annual	•	1981–2023
Food	crop production, fertilizer, irrigated area	_		provincial, annual	•	1981–2023
Water demand	domestic (NLWUD) (Zhou et al.		•	prefectural, annual	•	1965–2013 1981–2023
Water supply	runoff, streamflow, water stress	<ul> <li>China Natural Runoff Dataset (CNRD) (Gou et al., 2021),</li> <li>Gauge-based Natural Streamflow Dataset (Miao et al., 2022)</li> <li>Yellow River Water Resources Bulletin (YRCCMWR, 2020)</li> </ul>		0.25° grid, Monthly 0.25° grid, annual provincial, annual	•	1961–2018 1961–2018 1998–2022
Sediment	sediment load	• Yellow River Water Resources Bulletin (YRCCMWR, 2020)	•	provincial, annual	•	1998–2022
Land	<ul> <li>China land use remote sensing monitoring dataset (CNLUCC) (Xu et al., 2018)</li> <li>Land grassland, wetland, settlement</li> <li>Long-term global land surface satellite fractional vegetation cover product (Jia et al., 2015, 2019)</li> </ul>		•	1 km grid, annual	•	1980, 1990, 1995, 2000, 2005, 2010, 2015, 2020
Carbon	fossil fuel carbon emissions, net primary productivity	emissions, net Accounts and Datasets orimary (Shan et al., 2018),		Provincial, annual 5 km grid, 8 day	•	1997–2021 1981–2018





		Productivity Products (GVPP) (Cui et al., 2016; Wang et al., 2020a; Yu et al., 2018)				
Climate	temperature, precipitation, CO2 concentration, potential evapotranspiration and precipitation intensity	Agency (EEA, 2019),	•	0.25° grid, Annual Global, Annual Meteorolog ical stations, Monthly	•	1961–2020 1800-2020 1956-2018

\* Listed are some typical variables of each sector

## 418 **3 Model validation and application**

## 419 3.1 Historical model validation

420

421

422

423

424

425

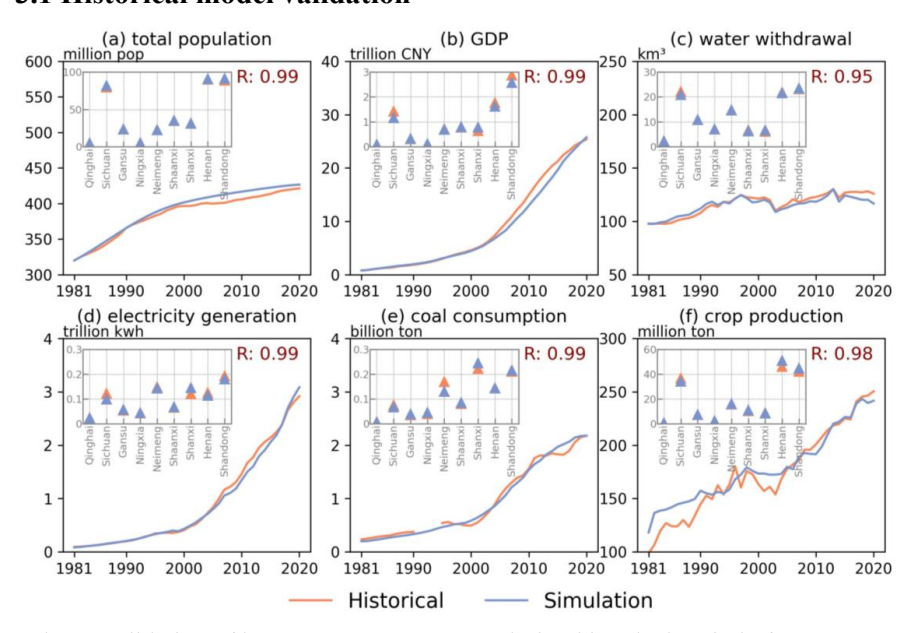


Fig.11 Validation of human system processes during historical period of 1981-2020.
(a) total population in *Population* sector; (b) GDP in *Economy* sector; (c) water withdrawal in *Water Demand* sector; (d) electricity generation and (e) coal consumption in *Energy* sector; (f) crop production in *Food* sector. Pink triangles in the

upper left sub-image represents the average of historical and simulation value in

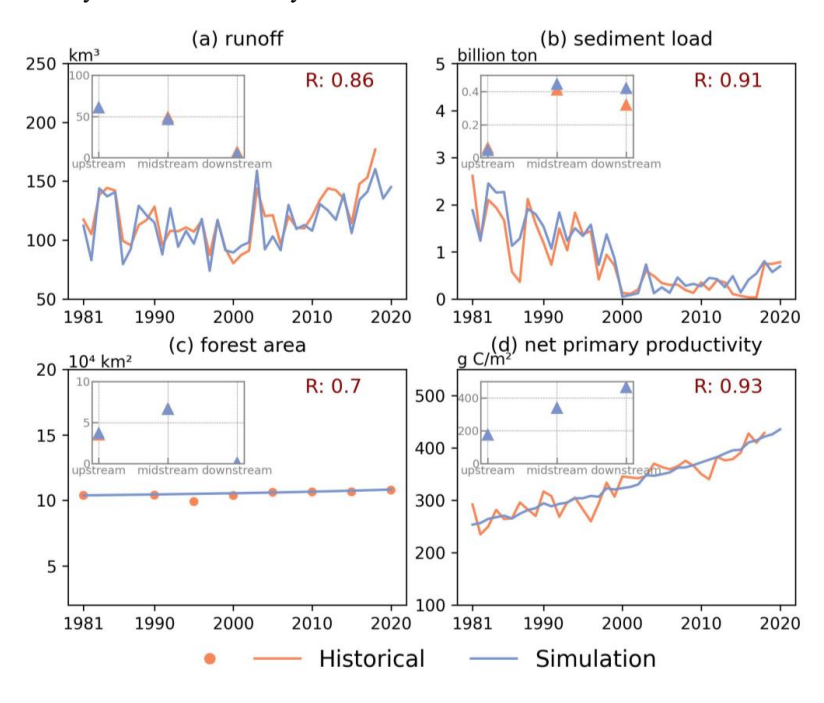




1981-2020 of each province in the YRB.

We compared model performance during the historical period (1981–2020) against historical data. These data are sourced from multiple channels, including statistical yearbooks, hydrological stations, remote sensing observations, and outputs from other models (Table S3).

For human sectors, the simulation accuracy of selected key variables from each sector is consistently high (R > 0.95), including total population, gross domestic product (GDP), water withdrawal, electricity generation, coal consumption, and crop production across the nine provinces. However, the accuracy varies among provinces, particularly for GDP, electricity generation, coal consumption, and crop production. In general, Shanxi exhibits lower simulation accuracy compared to the others. Among all sectors, the greatest uncertainty arises in simulating coal consumption, because the absence of a clear historical trend results in poor fitting performance. Nevertheless, the model performs reasonably well in the human sectors, effectively capturing the historical dynamics of human systems in the YRB.







443 2020. (a) runoff in *Water Supply* sector; (b) sediment load in *Sediment* sector; (c) 444 forest area in Land sector, and the historical dataset is discontinuous; (d) net primary 445 productivity in Carbon sector. Pink triangles in the upper left sub-image represents 446 the average of historical and simulation value in 1981-2020 of each sub-basin in the 447 YRB. 448 For natural sectors, the simulation accuracy for runoff, sediment load, forest area, 449 and NPP in the YRB is relatively high (R > 0.7). At the sub-basin level, the overall performance is satisfactory; however, the model shows lower accuracy in simulating 450 451 sediment transport in the mid- and downstream. Compared to the human sectors, the 452 natural sectors generally exhibit lower correlations with historical data, largely due to 453 the simplifications required when modeling physically complex natural processes. 454 Nevertheless, the model is still capable of capturing the historical dynamics of natural 455 processes in the YRB. 456 3.2 Model application for future projection 457 3.2.1 Future baseline scenario 458 The future baseline scenario represents a trajectory in which existing plans and 459 policies continue to operate without substantial changes in external environments. The development of the baseline scenario primarily relies on variables from the *Population*, 460 461 Economy, Water Demand, and Land sector based on available government planning documents, historical trends, and other projections (Table 2). Future climate data (2015-462 2100) are from the ensemble mean of 11 CMIP6 models (ACCESS-CM2, CESM2, 463 CMCC-ESM2, GFDL-ESM4, INM-CM4-8, INM-CM5-0, IPSL-CM6A-LR, MIROC6, 464 MRI-ESM2-0, UKESM1-0-LL, HadGEM-GC31-LL) 465 and (available https://cds.climate.copernicus.eu/datasets/projections-cmip6?tab=download) for the 466 467 SSP 2-4.5 because this scenario aligns more closely with the climate trends in the YRB. 468 To ensure temporal consistency, CMIP6 historical climate data (1981-2014) were used 469 instead of observed historical records. We run the model under the future baseline

Fig. 12 Validation of the natural system processes during historical period of 1981-





- 470 scenario to project the evolution of CHANS in the basin from 2021 to 2100 (see
- 471 Supporting Information S5 for details of scenario design).

Table 2 Settings of key variables in the future baseline scenario

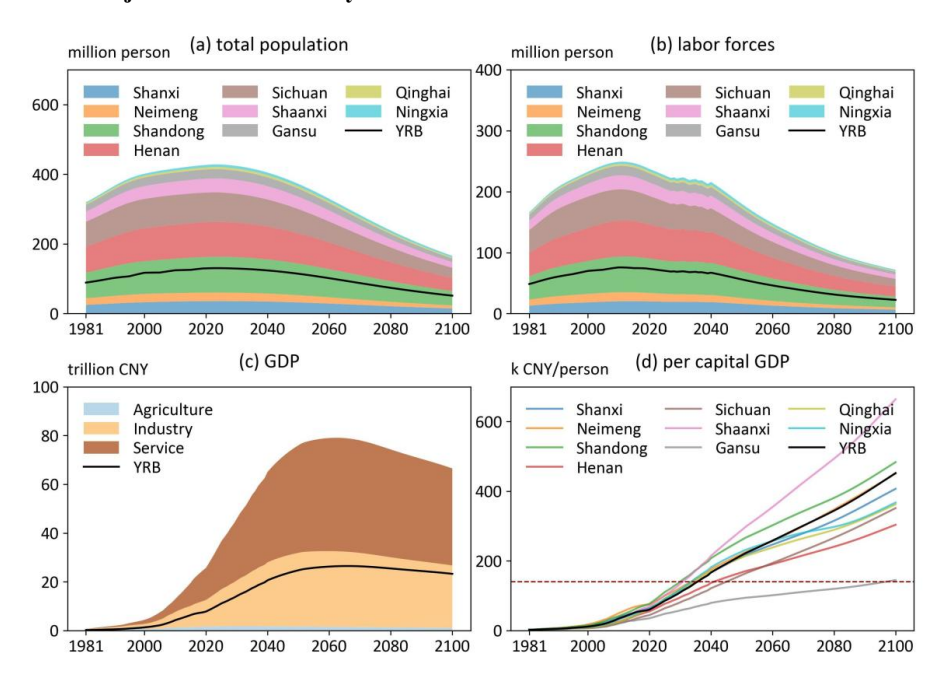
Sector	Variables		Future baseline				
	Total fertility	•	2024 United Nations Population Projection				
	Gender ratio	•	2024 United Nations Population Projection				
	Average years of	•	The national maximum in 2023 (Germany)				
Population	schooling		as the upper limit				
	Urban and rural	•	Analysis and Forecast of Urbanization				
	population ratio		Trends in China's Modernization by 2020				
	• Labor force	•	Delay retirement age				
		•	Projected provincial-level energy structure				
	Electricity generation		meeting China's carbon peaking and carbo				
Energy	sources ratio		neutrality goals (Li et al., 2024)				
		•	Irrigation water use intensity declines				
	Irrigation intensity		linearly (1%/yr) to its minimum value.				
	Industry, service,	•	Industry, service and livestock water use				
Water Demai	nd livestock water use		intensity declines linearly (1%/yr) to its				
	intensity		minimum value.				
		•	Minimum cropland area above the red line				
r J	Land use area		for cropland protection.				
Land	Land use area	•	Other lands are allowed to be fully				
			converted into other categories.				
	Temperature,						
Climata	Precipitation, Potential	_	CCD 2.4.5 CMID (				
Climate	evapotranspiration,		SSP 2-4.5 —— CMIP 6				
	precipitation intensity,						





### CO<sub>2</sub> concentration,

## 3.2.2 Projection of CHANS dynamics in future baseline scenario



474

475

476

477

478479

473

Fig.13 Changes in key variables of the *Population* and *Economy* sector in the future baseline scenario: (a) the total population, (b) the total labor forces, (c) the gross output of agriculture, industry, and service, and the total gross domestic output, (d) the per capital GDP in nine provinces and YRB.

The model simulates human and natural system dynamics under the future

baseline scenario and produces outputs for nine provinces and their corresponding areas within the YRB. The simulation results are reported either at the provincial level (nine provinces) for human system sectors or at the basin level (basin boundary) for natural system sectors. The total population in the nine provinces and the YRB is projected to peak in 2023 and 2024, at 428 million and 131 million, respectively, driven by declining

fertility rates. The labor force peaks earlier, reaching 249 million in the nine provinces in 2011 and 76 million in the YRB in 2010. After 2025, the labor force is projected to

487 increase again due to the delayed retirement policy. GDP in the nine provinces is





expected to increase until a peak in 2062, at 79 trillion CNY (three times the 2020 level, in 2020 constant prices), under the influence of a labor force decline, with the YRB reaching its peak four years later. In contrast to total GDP, per capita GDP in all regions is projected to continue rising throughout the future period. Although all provinces demonstrate improvements in economic status and living standards, considerable regional disparities persist. Among the nine provinces, Shaanxi demonstrates the largest growth in average per capita GDP from 2021 to 2100 relative to the historical period (1981-2020), with a more than sixteenfold increase, while the YRB as a whole shows an over twelvefold increase.

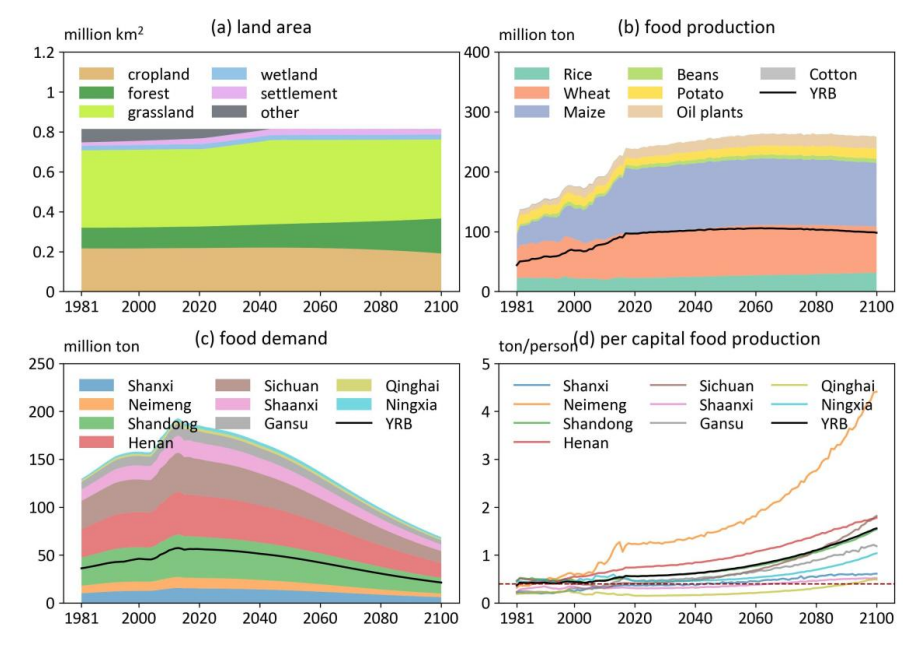


Fig.14 Land and food in the future baseline scenario. (a) land area in the YRB; (b-d) food production of seven crop types, food demand and per capital food production in nine provinces and the YRB, red dotted line represents the 0.4 tons international food security threshold.

Under the future baseline scenario, land use patterns remain relatively stable based on historical trends, as no new land policies are introduced and cropland area needs to stay above the red line. The forest area is projected to increase gradually, reaching 62%





above the 2021 level by 2100, while the cropland area is expected continue declining, falling 12% below the 2021 level. Total crop production in nine provinces and YRB is projected to peak in 2079 and 2062, respectively, driven by the combined effects of declining cropland area and increasing crop yields. Food demand in both the nine provinces and the YRB as a whole peaked in 2013 (192 million tons and 57 million tons, respectively), largely driven by population dynamics. In the future, per capita food production in the YRB is projected to consistently exceed the international food security threshold of 0.4 tons per person. However, in certain years, provinces such as Qinghai and Shaanxi could fall below this standard.

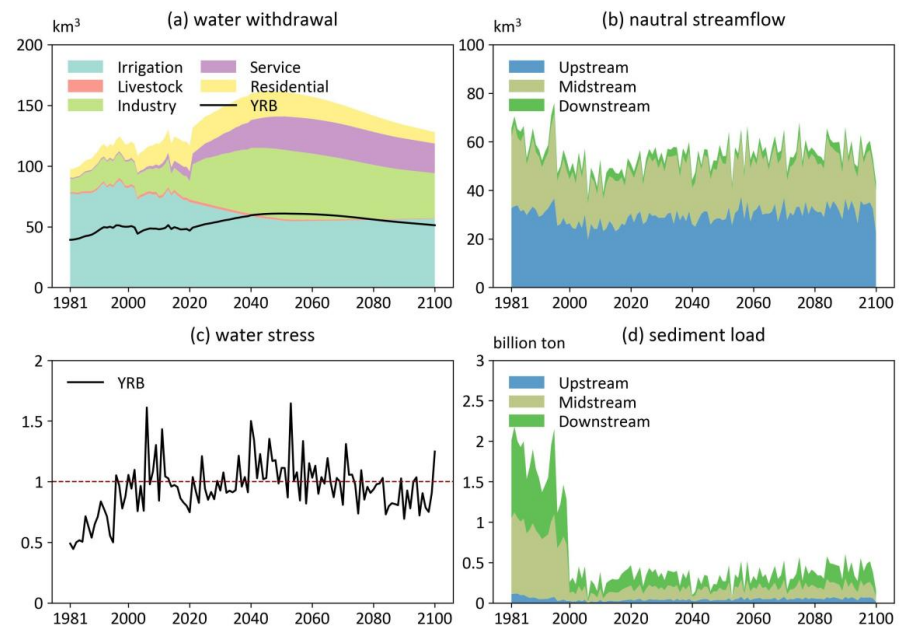


Fig.15 Water demand and supply in the future baseline scenario. (a) water withdrawal across five water-use sectors in nine provinces and the YRB; (b) natural streamflow in up-, mid- and downstream; (c) water stress in the YRB, red dotted line represents the water security threshold; (d) sediment load in the up-, mid- and downstream.

Total water withdrawal in the nine provinces and the YRB is projected to peak in 2047 and 2051, reaching 162 km<sup>3</sup> and 61 km<sup>3</sup>, respectively. Irrigation water withdrawal is expected to decline, driven by reductions in cropland area and irrigation intensity, the





latter resulting from improvements in irrigation efficiency assumed in the scenario. Peaks in residential, industrial, service, and livestock water withdrawals are primarily associated with projected peaks in population and GDP. Natural streamflow is projected to follow a fluctuating upward trend, with the future annual mean nearly identical to the historical average (a 0.7% increase), and the largest increase occurring in the upstream region (8%). Considering the ecological flow requirement of 18.7 km<sup>3</sup> (YRCCMWR, 2015), water stress (calculated as water consumption divided by (natural discharge - ecological flow)) is expected to decline in the latter half of the century, largely due to the peak and subsequent reduction in water withdrawal. However, overall water stress is projected to exceed historical levels in 2041 and will fall below 1 in 54% of the years, reflecting mitigation of persistent human—water tensions and future tradeoffs between ecological and human water use. As a result of reduced actual streamflow, sediment transport in the Yellow River is projected to decline sharply, with a 63% decrease in sediment load relative to the historical period.

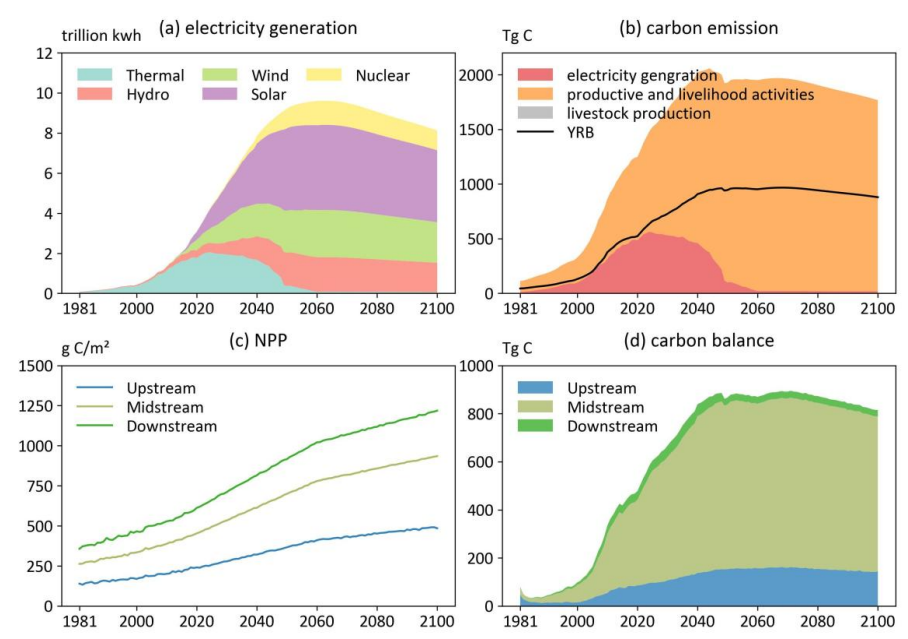


Fig.16 Electricity and carbon in the future baseline scenario. (a) the electricity generation from five sources in nine provinces; (b) carbon emission from three





539 sources in nine provinces and the YRB; (c-d) the net primary productivity and carbon 540 balance in the up-, mid-, and downstream. 541 Since the energy system is transitioning to carbon neutrality goals under the future 542 baseline scenario, thermal power generation is projected to decline sharply, while clean 543 energy (hydropower, wind, solar, and nuclear) will become the dominant source for 544 electricity generation. The large-scale adoption of clean energy will lead to a peak in 545 carbon emissions from electricity generation in 2024. In contrast, emissions from 546 productive and livelihood activities are projected to rise substantially over time, with 547 total human emissions in the YRB reaching a peak in 2044. NPP is anticipated to increase markedly in response to CO2 concentration increase. Although the carbon 548 549 balance of the YRB has remained positive (net carbon source), it is expected to 550 gradually decline after 2071, indicating that the basin's ecosystems alone cannot fully 551 offset human-induced carbon emissions. 552 The above projections of future baseline scenarios highlight persistent challenges 553 to achieving sustainable development in the YRB, underscoring the need for integrated policy responses to address these challenges. Priority should be given to enhancing 554 555 water-use efficiency and establishing adaptive water resource allocation mechanisms 556 that balance ecological and human water needs. Sediment management strategies, which combine ecological restoration with hydraulic regulation, are necessary to 557 558 maintain river stability and delta health. To counter the decline in labor force, policies 559 should promote industrial upgrading and technological innovation. Strengthening the basin's carbon mitigation capacity requires accelerating the clean energy transition and 560 561 expanding ecological restoration to enhance carbon sequestration. Finally, a multisectoral, CHANS-based governance framework should be established to coordinate 562 563 water, land, energy, and carbon management, enabling evidence-based scenario 564 analysis and adaptive policy design for long-term sustainability.

4 Discussion and conclusions

565566

568569

570

571

572

573

574

575

576577

578

579580

581

582

583

584

585 586

587

588 589

590

591

592

593

594





considerations in translating a conceptual framework into a functioning model. The framework focuses on human-water interactions in the YRB, integrating bidirectional feedback between human and natural processes. SD was chosen to implement the framework, as it effectively captures feedback, non-linear relationships, and crosssectoral linkages within complex human-natural systems, while remaining practical and straightforward to use. For quantitative representation of human-natural processes, we prefer theoretical methods that incorporate key interactions within the system suitable for implementation using SD. For example, the Budyko framework connects the Land, Climate, Water Demand, and Water Supply sectors. Relative to distributed hydrological models, it offers lower computational complexity and reduced data requirements. The Cobb-Douglas production function links the Population and Economy sectors. Compared with Computable General Equilibrium models (Fujimori et al., 2014), it is simpler to construct and requires fewer parameters and data inputs. When no suitable theoretical framework/method is available to describe a process, we rely on empirical relationships derived from historical data. For example, crop yields are estimated using fitted relationships between climate variables, fertilizer application, and historical yields. For processes that cannot be represented through empirical functions, we apply literature-based estimates to obtain approximate quantitative relationships, such as fossil fuel emission factors. For processes influenced by external drivers that cannot be endogenously expressed within the model, we quantify them using exogenous parameters derived from historical statistics, such as water intensity. Given the heterogeneous human-natural interactions in the YRB, we represent all processes at the provincial and sub-basin scales using scale-specific parameters, except where parameters or data at these levels are unavailable. The CHANS-SD-YRB model explicitly couples multiple human and natural sectors, enabling a more integrated representation of feedbacks across population, economy, energy, food, water, sediment, land, carbon, and climate. Unlike models that focus on specific sectors or isolated subsystems—such as eco-hydrological models and

596

597

598599

600

601

602

603

604 605

606

607 608

609

610

611

612

613 614

615

616 617

618 619

620

621

622





sediment transport models, which may well capture individual processes but cannot represent the complex human-nature interactions driving system dynamics. Our model's comprehensive coupling broadens its scope of application to address complex regional CHANS challenges and provides practical guidance for sustainable development. The CHANS-SD-YRB model serves as a comprehensive platform for conducting system dynamics prediction, scenario analysis, policy evaluation, and optimization, to alleviate human-water conflicts, ensure food security, and achieve long-term sustainability. For example, analysis of the impacts of the 1987 Yellow River water allocation policy (Song et al., 2024) offer valuable insights for adjusting interprovincial water distribution to promote sustainable water governance; assessment of ecological restoration policies (Li et al., 2015) can guide future ecological engineering; spatiotemporal dynamics of future water gaps can serve as a valuable reference for planning inter-basin water transfers. The model's flexibility also allows for the incorporation of additional feedback, for example, linking water scarcity to industrial output or climate warming to agricultural productivity. These could include the effects of global warming on human health (Yin et al., 2023a) and economic activities (Nordhaus, 2017), water constraints on production, dietary shifts influencing carbon emissions and land use (Ren et al., 2023), and the trade-offs between carbon mitigation and food security (Xu et al., 2022). Nevertheless, the model remains subject to further refinement. The current simplifications of natural processes could be replaced with more sophisticated models to enhance simulation accuracy. For instance, the YRB hydrological processes involve highly complex human interventions, including reservoir, conservation, and revegetation projects (Wang et al., 2025). The refined runoff simulations by distributed hydrological models improve water supply assessments through their better characterization of spatial heterogeneity in soil, precipitation, and snowmelt (Cong et al., 2009). The model's spatial and temporal resolutions are relatively coarse due to the inherent mismatch in spatiotemporal scales between human and natural processes. The





623 scale at which we make the model represents a practical compromise, constrained by 624 data availability and aligned with the study's objectives. Simulations at finer scales (e.g., 625 monthly, daily, or gridded) would enhance the representation of natural processes (e.g., hydrological processes, land use changes, and food production) and the associated 626 627 spatiotemporal heterogeneity (e.g., daily simulations can assess the impacts of extreme 628 weather). However, it may also exacerbate the scale mismatch with socioeconomic 629 processes, making it challenging to analyze cross-sectoral dynamics. Technically, the 630 inherent limitations of the SD software restrict the model's ability to represent temporal 631 fluctuations and spatial variations. To overcome this, transitioning from the VENSIM platform to a code-based implementation will be necessary, which would also facilitate 632 633 coupling with other models. Future research should prioritize these improvements to 634 strengthen both the performance and applicability of the model. Overall, the CHANS-SD-YRB model fills the gap in CHANS modeling for the 635 636 YRB. It integrates the dynamics of ten interconnected sectors: *Population, Economy*, 637 Energy, Food, Water Demand, Water Supply, Sand, Land, Carbon, and Climate, achieving reciprocal feedback between human and natural systems. This model can 638 639 serve as a robust tool to inform policy decisions that influence the evolution of coupled 640 human-natural systems and to explore pathways for optimizing these systems toward 641 sustainability. Furthermore, the modeling process provides valuable experience for 642 regional CHANS modeling and contributes to advancing the broader development of 643 CHANS models at the regional scale. 644 Code and data availability 645 The CHANS-SD-YRB V1.0 model (Vensim DSS format), along with the input data and simulation outputs used in this study, are openly accessible at 646 647 https://doi.org/10.5281/zenodo.17568963 (Sang, 2025). **Author contributions** 648 649 Conceptualization: YL, SS<sup>1</sup>, BF. Data curation: SS<sup>1</sup>. Formal analysis: SS<sup>1</sup>. 650 Funding acquisition: BF, YL. Investigation: YL, SS<sup>1</sup>. Methodology: SS<sup>1</sup>, YL, BF.





- Project administration: YL. Resources: YL. Software: SS<sup>1</sup>, SZ, LY. Supervision: YL,
- 652 BF. Validation: SS<sup>1</sup>, SZ, LY. Visualization: SS<sup>1</sup>. Writing original draft: SS<sup>1</sup>. Writing –
- review and editing: SS<sup>1</sup>, YL, SW, YXL, XTW, SS<sup>2</sup>, WZ, XHW. (Note: SS<sup>1</sup> refers to
- 654 Shan Sang, and SS<sup>2</sup> refers to Shuang Song, to distinguish between authors with identical
- 655 initials.)

## 656 Competing interests

The authors declare that they have no conflict of interest.

## Acknowledgements

- We thank Dr. Weishuang Qu for developing the Threshold 21 model in the
- 660 Millennium Institute that inspired this study, and also for his and Dr. Haiyan Jiang's
- generous help with the CHANS-SD-YRB modeling. We also thank the data support
- 662 from National Earth System Science Data Center, National Science & Technology
- Infrastructure of China (http://www.geodata.cn).

## 664 Financial support

- This study is supported by the National Natural Science Foundation of China
- 666 (Grant No. 42041007), and the Fundamental Research Funds for the Central
- 667 Universities.

#### 668 **References:**

- 669 Akhtar, M. K., Wibe, J., Simonovic, S. P., and MacGee, J.: Integrated assessment model
- of society-biosphere-climate-economy-energy system, Environmental Modelling &
- 671 Software, 49, 1–21, https://doi.org/10.1016/j.envsoft.2013.07.006, 2013.
- Allen, C., Metternicht, G., Wiedmann, T., and Pedercini, M.: Greater gains for Australia
- by tackling all SDGs but the last steps will be the most challenging, Nat Sustain, 2,
- 674 1041–1050, https://doi.org/10.1038/s41893-019-0409-9, 2019.
- 675 Baldos, U. L. C., Chepeliev, M., Cultice, B., Huber, M., Meng, S., Ruane, A. C., Suttles,
- 676 S., and van der Mensbrugghe, D.: Global-to-local-to-global interactions and climate
- 677 change, Environ. Res. Lett., 18, 053002, https://doi.org/10.1088/1748-9326/acc95c,
- 678 2023.
- 679 Breach, P. A. and Simonovic, S. P.: ANEMI3: An updated tool for global change
- 680 analysis, PLoS ONE, 16, e0251489, https://doi.org/10.1371/journal.pone.0251489,
- 681 2021.





- 682 Changming, L. and Shifeng, Z.: Drying up of the yellow river: its impacts and counter-
- 683 measures, Mitigation and Adaptation Strategies for Global Change, 7, 203-214,
- 684 https://doi.org/10.1023/A:1024408310869, 2002.
- 685 Cheng, Y., Huang, M., Lawrence, D. M., Calvin, K., Lombardozzi, D. L., Sinha, E.,
- 686 Pan, M., and He, X.: Future bioenergy expansion could alter carbon sequestration
- 687 potential and exacerbate water stress in the United States, Science Advances, 8,
- 688 eabm8237, https://doi.org/10.1126/sciadv.abm8237, 2022.
- 689 Clark, M. P., Fan, Y., Lawrence, D. M., Adam, J. C., Bolster, D., Gochis, D. J., Hooper,
- 690 R. P., Kumar, M., Leung, L. R., Mackay, D. S., Maxwell, R. M., Shen, C., Swenson, S.
- 691 C., and Zeng, X.: Improving the representation of hydrologic processes in Earth System
- 692 Models, Water Resources Research, 51, 5929-5956,
- 693 https://doi.org/10.1002/2015WR017096, 2015.
- 694 Cobb, C. W. and Douglas, P. H.: A theory of production, The American Economic
- 695 Review, 18, 139–165, 1928.
- 696 Cong, Z., Yang, D., Gao, B., Yang, H., and Hu, H.: Hydrological trend analysis in the
- 697 Yellow River basin using a distributed hydrological model, Water Resources Research,
- 698 45, 2008WR006852, https://doi.org/10.1029/2008WR006852, 2009.
- 699 Cui, T., Wang, Y., Sun, R., Qiao, C., Fan, W., Jiang, G., Hao, L., and Zhang, L.:
- 700 Estimating Vegetation Primary Production in the Heihe River Basin of China with
- 701 Multi-Source and Multi-Scale Data, PLOS ONE, 11, e0153971,
- 702 https://doi.org/10.1371/journal.pone.0153971, 2016.
- 703 Davies, E. G. R. and Simonovic, S. P.: ANEMI: a new model for integrated assessment
- of global change, Interdisciplinary Environmental Review, 2011.
- 705 Di Vittorio, A. V., Sinha, E., Hao, D., Singh, B., Calvin, K. V., Shippert, T., Patel, P.,
- and Bond-Lamberty, B.: E3SM-GCAM: A Synchronously Coupled Human Component
- 707 in the E3SM Earth System Model Enables Novel Human-Earth Feedback Research,
- 708 Journal of Advances in Modeling Earth Systems, 17, e2024MS004806,
- 709 https://doi.org/10.1029/2024MS004806, 2025.
- 710 Dobbs, G. R., Liu, N., Caldwell, P. V., Miniat, C. F., Sun, G., Duan, K., and Bolstad, P.
- 711 V.: Inter-basin surface water transfers database for public water supplies in
- 712 conterminous United States, 1986–2015, Sci Data, 10, 255,
- 713 https://doi.org/10.1038/s41597-023-02148-5, 2023.
- 714 Dottori, F., Szewczyk, W., Ciscar, J.-C., Zhao, F., Alfieri, L., Hirabayashi, Y., Bianchi,
- A., Mongelli, I., Frieler, K., Betts, R. A., and Feyen, L.: Increased human and economic
- 716 losses from river flooding with anthropogenic warming, Nature Clim Change, 8, 781–





- 717 786, https://doi.org/10.1038/s41558-018-0257-z, 2018.
- 718 EEA: Trends in atmospheric concentrations of CO2 (ppm), CH4 (ppb) and N2O (ppb),
- 719 between 1800 and 2017, 2019.
- 720 Feng, X., Fu, B., Piao, S., Wang, S., Ciais, P., Zeng, Z., Lü, Y., Zeng, Y., Li, Y., Jiang,
- 721 X., and Wu, B.: Revegetation in China's Loess Plateau is approaching sustainable water
- 722 resource limits, Nature Clim Change, 6, 1019–1022,
- 723 https://doi.org/10.1038/nclimate3092, 2016.
- 724 Feng, Y. and Zhu, A.: Spatiotemporal differentiation and driving patterns of water
- 725 utilization intensity in Yellow River Basin of China: Comprehensive perspective on the
- 726 water quantity and quality, Journal of Cleaner Production, 369, 133395,
- 727 https://doi.org/10.1016/j.jclepro.2022.133395, 2022.
- 728 Fu, B. and Li, Y.: Bidirectional coupling between the Earth and human systems is
- 729 essential for modeling sustainability, National Science Review, 3, 397-398,
- 730 https://doi.org/10.1093/nsr/nww094, 2016.
- Fu, B., Liu, Y., Lü, Y., He, C., Zeng, Y., and Wu, B.: Assessing the soil erosion control
- service of ecosystems change in the Loess Plateau of China, Ecological Complexity, 8,
- 733 284–293, https://doi.org/10.1016/j.ecocom.2011.07.003, 2011.
- 734 Fu, B., Liu, Y., and Meadows, M. E.: Ecological restoration for sustainable
- 735 development in China, National Science Review, 10, nwad033,
- 736 https://doi.org/10.1093/nsr/nwad033, 2023.
- 737 Fujimori, S., Masui, T., and Matsuoka, Y.: Development of a global computable general
- equilibrium model coupled with detailed energy end-use technology, Applied Energy,
- 739 128, 296–306, https://doi.org/10.1016/j.apenergy.2014.04.074, 2014.
- 740 Fujimori, S., Wu, W., Doelman, J., Frank, S., Hristov, J., Kyle, P., Sands, R., van Zeist,
- 741 W.-J., Havlik, P., Domínguez, I. P., Sahoo, A., Stehfest, E., Tabeau, A., Valin, H., van
- 742 Meijl, H., Hasegawa, T., and Takahashi, K.: Land-based climate change mitigation
- measures can affect agricultural markets and food security, Nat Food, 3, 110-121,
- 744 https://doi.org/10.1038/s43016-022-00464-4, 2022.
- Gou, J., Miao, C., Samaniego, L., Xiao, M., Wu, J., and Guo, X.: CNRD v1.0: A High-
- 746 Quality Natural Runoff Dataset for Hydrological and Climate Studies in China, Bulletin
- 747 of the American Meteorological Society, 102, E929–E947,
- 748 https://doi.org/10.1175/BAMS-D-20-0094.1, 2021.
- 749 Hasegawa, T., Sakurai, G., Fujimori, S., Takahashi, K., Hijioka, Y., and Masui, T.:
- 750 Extreme climate events increase risk of global food insecurity and adaptation needs,
- 751 Nat Food, 2, 587–595, https://doi.org/10.1038/s43016-021-00335-4, 2021.





- 752 Hyun, J.-Y., Huang, S.-Y., Yang, Y.-C. E., Tidwell, V., and Macknick, J.: Using a
- 753 coupled agent-based modeling approach to analyze the role of risk perception in water
- 754 management decisions, Hydrology and Earth System Sciences, 23, 2261-2278,
- 755 https://doi.org/10.5194/hess-23-2261-2019, 2019.
- 756 Jain, S., Mindlin, J., Koren, G., Gulizia, C., Steadman, C., Langendijk, G. S., Osman,
- 757 M., Abid, M. A., Rao, Y., and Rabanal, V.: Are We at Risk of Losing the Current
- 758 Generation of Climate Researchers to Data Science?, AGU Advances, 3,
- 759 e2022AV000676, https://doi.org/10.1029/2022AV000676, 2022.
- 760 Jia, K., Liang, S., Liu, S., Li, Y., Xiao, Z., Yao, Y., Jiang, B., Zhao, X., Wang, X., Xu,
- 761 S., and Cui, J.: Global Land Surface Fractional Vegetation Cover Estimation Using
- 762 General Regression Neural Networks From MODIS Surface Reflectance, IEEE
- 763 Transactions on Geoscience and Remote Sensing, 53, 4787-4796,
- 764 https://doi.org/10.1109/TGRS.2015.2409563, 2015.
- 765 Jia, K., Yang, L., Liang, S., Xiao, Z., Zhao, X., Yao, Y., Zhang, X., Jiang, B., and Liu,
- 766 D.: Long-Term Global Land Surface Satellite (GLASS) Fractional Vegetation Cover
- 767 Product Derived From MODIS and AVHRR Data, IEEE Journal of Selected Topics in
- 768 Applied Earth Observations and Remote Sensing, 12, 508-518,
- 769 https://doi.org/10.1109/JSTARS.2018.2854293, 2019.
- Jiang, H., Simonovic, S. P., and Yu, Z.: ANEMI\_Yangtze v1.0: a coupled human-
- 771 natural systems model for the Yangtze Economic Belt model description, Geosci.
- 772 Model Dev., 26, 2022.
- 773 Kemei, Z., Rotich, T., and Bitok, J.: Modelling population dynamics using age-
- 774 structured system of partial differential equations, IJAMR, 13, 110-116,
- 775 https://doi.org/10.14419/m81azj37, 2024.
- 776 Li, M., Shan, R., Abdulla, A., Virguez, E., and Gao, S.: The role of dispatchability in
- 777 China's power system decarbonization, Energy Environ. Sci., 17, 2193–2205,
- 778 https://doi.org/10.1039/D3EE04293F, 2024.
- 779 Li, X., Cheng, G., Lin, H., Cai, X., Fang, M., Ge, Y., Hu, X., Chen, M., and Li, W.:
- 780 Watershed System Model: The Essentials to Model Complex Human-Nature System at
- 781 the River Basin Scale, Journal of Geophysical Research: Atmospheres, 123, 3019–3034,
- 782 https://doi.org/10.1002/2017JD028154, 2018.
- 783 Li, X., Zhang, L., Zheng, Y., Yang, D., Wu, F., Tian, Y., Han, F., Gao, B., Li, H., Zhang,
- 784 Y., Ge, Y., Cheng, G., Fu, B., Xia, J., Song, C., and Zheng, C.: Novel hybrid coupling
- 785 of ecohydrology and socioeconomy at river basin scale: A watershed system model for
- 786 the Heihe River basin, Environmental Modelling & Software, 141, 105058,
- 787 https://doi.org/10.1016/j.envsoft.2021.105058, 2021.





- 788 Li, Y., Sang, S., Mote, S., Rivas, J., and Kalnay, E.: Challenges and opportunities for
- 789 modeling coupled human and natural systems, National Science Review, 10, nwad054,
- 790 https://doi.org/10.1093/nsr/nwad054, 2023.
- 791 Li, Z., Liu, X., Niu, T., Kejia, D., Zhou, Q., Ma, T., and Gao, Y.: Ecological Restoration
- and Its Effects on a Regional Climate: The Source Region of the Yellow River, China,
- 793 Environ. Sci. Technol., 49, 5897–5904, https://doi.org/10.1021/es505985q, 2015.
- 794 Liu, C., Golding, D., and Gong, G.: Farmers' coping response to the low flows in the
- 795 lower Yellow River: A case study of temporal dimensions of vulnerability, Global
- 796 Environmental Change, 18, 543–553, https://doi.org/10.1016/j.gloenvcha.2008.09.002,
- 797 2008.
- 798 Liu, J.: Integration across a metacoupled world, E&S, 22, art29,
- 799 https://doi.org/10.5751/ES-09830-220429, 2017.
- 800 Liu, J., Dietz, T., Carpenter, S. R., Alberti, M., Folke, C., Moran, E., Pell, A. N.,
- 801 Deadman, P., Kratz, T., Lubchenco, J., Ostrom, E., Ouyang, Z., Provencher, W.,
- 802 Redman, C. L., Schneider, S. H., and Taylor, W. W.: Complexity of Coupled Human
- 803 and Natural Systems, Science, 317, 1513-1516,
- 804 https://doi.org/10.1126/science.1144004, 2007.
- 805 MAARA: China Agriculture Yearbook,
- https://data.cnki.net/yearBook?type=type&code=A, 2020.
- 807 Miao, C., Kong, D., Wu, J., and Duan, Q.: Functional degradation of the water-
- 808 sediment regulation scheme in the lower Yellow River: Spatial and temporal analyses,
- 809 Science of The Total Environment, 551–552, 16–22,
- 810 https://doi.org/10.1016/j.scitotenv.2016.02.006, 2016.
- 811 Miao, C., Gou, J., Fu, B., Tang, Q., Duan, Q., Chen, Z., Lei, H., Chen, J., Guo, J.,
- 812 Borthwick, A. G. L., Ding, W., Duan, X., Li, Y., Kong, D., Guo, X., and Wu, J.: High-
- 813 quality reconstruction of China's natural streamflow, Science Bulletin, 67, 547–556,
- 814 https://doi.org/10.1016/j.scib.2021.09.022, 2022.
- 815 Monier, E., Paltsev, S., Sokolov, A., Chen, Y.-H. H., Gao, X., Ejaz, Q., Couzo, E.,
- 816 Schlosser, C. A., Dutkiewicz, S., Fant, C., Scott, J., Kicklighter, D., Morris, J., Jacoby,
- 817 H., Prinn, R., and Haigh, M.: Toward a consistent modeling framework to assess multi-
- 818 sectoral climate impacts, Nat Commun, 9, 1–8, https://doi.org/10.1038/s41467-018-
- 819 02984-9, 2018.
- 820 Motesharrei, S., Rivas, J., Kalnay, E., Asrar, G. R., Busalacchi, A. J., Cahalan, R. F.,
- 821 Cane, M. A., Colwell, R. R., Feng, K., Franklin, R. S., Hubacek, K., Miralles-Wilhelm,
- 822 F., Miyoshi, T., Ruth, M., Sagdeev, R., Shirmohammadi, A., Shukla, J., Srebric, J.,





- 823 Yakovenko, V. M., and Zeng, N.: Modeling sustainability: population, inequality,
- 824 consumption, and bidirectional coupling of the Earth and Human Systems, National
- 825 Science Review, 3, 470–494, https://doi.org/10.1093/nsr/nww081, 2016.
- 826 NBSC: China Energy Statistical Yearbook,
- https://data.cnki.net/yearBook?type=type&code=A, 2020a.
- 828 NBSC: China Population Census Yearbook,
- https://data.cnki.net/yearBook?type=type&code=A, 2020b.
- NBSC: China Statistical Yearbooks, https://www.stats.gov.cn/english/, 2020c.
- 831 Ning, X., Zhu, N., Liu, Y., and Wang, H.: Quantifying impacts of climate and human
- 832 activities on the grassland in the Three-River Headwater Region after two phases of
- 833 Ecological Project, Geography and Sustainability, 3, 164–176,
- 834 https://doi.org/10.1016/j.geosus.2022.05.003, 2022.
- 835 Nordhaus, W. D.: Revisiting the social cost of carbon, Proceedings of the National
- 836 Academy of Sciences, 114, 1518–1523, https://doi.org/10.1073/pnas.1609244114,
- 837 2017.
- 838 Qu, W., Shi, W., Zhang, J., and Liu, T.: T21 China 2050: A Tool for National Sustainable
- 839 Development Planning, Geography and Sustainability, 1, 33-46,
- 840 https://doi.org/10.1016/j.geosus.2020.03.004, 2020.
- 841 Rajah, J. K., Blanz, B., Kopainsky, B., and Schoenberg, W.: An endogenous modelling
- 842 framework of dietary behavioural change in the fully coupled human-climate FRIDA
- 843 v2.1 model, Geoscientific Model Development, 18, 5997–6022,
- 844 https://doi.org/10.5194/gmd-18-5997-2025, 2025.
- 845 Ren, M., Huang, C., Wu, Y., Deppermann, A., Frank, S., Havlík, P., Zhu, Y., Fang, C.,
- 846 Ma, X., Liu, Y., Zhao, H., Chang, J., Ma, L., Bai, Z., Xu, S., and Dai, H.: Enhanced
- food system efficiency is the key to China's 2060 carbon neutrality target, Nat Food, 4,
- 848 552–564, https://doi.org/10.1038/s43016-023-00790-1, 2023.
- Ristaino, J. B., Anderson, P. K., Bebber, D. P., Brauman, K. A., Cunniffe, N. J., Fedoroff,
- 850 N. V., Finegold, C., Garrett, K. A., Gilligan, C. A., Jones, C. M., Martin, M. D.,
- MacDonald, G. K., Neenan, P., Records, A., Schmale, D. G., Tateosian, L., and Wei, Q.:
- 852 The persistent threat of emerging plant disease pandemics to global food security,
- 853 Proceedings of the National Academy of Sciences, 118, e2022239118,
- 854 https://doi.org/10.1073/pnas.2022239118, 2021.
- 855 Rydzak, F., Obersteiner, M., Kraxner, F., Fritz, S., and McCallum, I.: FeliX3-Impact
- 856 Assessment Model: Systemic View across Societal Benefit Areas beyond Global Earth
- 857 Observation, Laxenburg: International Institute for Applied Systems Analysis (IIASA),





- 858 2013.
- 859 Sang, S.: CHANS-SD-YRB V1.0: A System Dynamics model of the coupled human-
- 860 natural systems for the Yellow River Basin (1.0.0), Zenodo,
- 861 https://doi.org/10.5281/zenodo.17568963, 2025.
- 862 Sang, S., Li, Y., Zong, S., Yu, L., Wang, S., Liu, Y., Wu, X., Song, S., Wang, X., and Fu,
- 863 B.: The modeling framework of the coupled human and natural systems in the Yellow
- 864 River Basin, Geography and Sustainability, 6, 100294,
- 865 https://doi.org/10.1016/j.geosus.2025.100294, 2025.
- 866 Shan, Y., Guan, D., Zheng, H., Ou, J., Li, Y., Meng, J., Mi, Z., Liu, Z., and Zhang, Q.:
- 867 China CO2 emission accounts 1997-2015, Sci Data, 5, 170201,
- 868 https://doi.org/10.1038/sdata.2017.201, 2018.
- 869 Song, S., Wen, H., Wang, S., Wu, X., Cumming, G. S., and Fu, B.: Quantifying the
- 870 effects of institutional shifts on water governance in the Yellow River Basin: A social-
- 871 ecological system perspective, Journal of Hydrology, 629, 130638,
- 872 https://doi.org/10.1016/j.jhydrol.2024.130638, 2024.
- 873 Vaidyanathan, G.: Integrated assessment climate policy models have proven useful,
- 874 with caveats, Proc. Natl. Acad. Sci. U.S.A., 118, e2101899118,
- 875 https://doi.org/10.1073/pnas.2101899118, 2021.
- Ventana Systems, Inc.: Vensim DSS (version 9.3), 2023.
- 877 Verburg, P. H., Dearing, J. A., Dyke, J. G., Leeuw, S. van der, Seitzinger, S., Steffen,
- 878 W., and Syvitski, J.: Methods and approaches to modelling the Anthropocene, Global
- 879 Environmental Change, 39, 328–340, https://doi.org/10.1016/j.gloenvcha.2015.08.007,
- 880 2016.
- 881 van Vliet, J.: Direct and indirect loss of natural area from urban expansion, Nat Sustain,
- 882 2, 755–763, https://doi.org/10.1038/s41893-019-0340-0, 2019.
- Waidelich, P., Batibeniz, F., Rising, J., Kikstra, J. S., and Seneviratne, S. I.: Climate
- damage projections beyond annual temperature, Nat. Clim. Chang., 14, 592-599,
- 885 https://doi.org/10.1038/s41558-024-01990-8, 2024.
- 886 Wang, M., Sun, R., Zhu, A., and Xiao, Z.: Evaluation and Comparison of Light Use
- 887 Efficiency and Gross Primary Productivity Using Three Different Approaches, Remote
- 888 Sensing, 12, 1003, https://doi.org/10.3390/rs12061003, 2020a.
- Wang, S., Fu, B., Piao, S., Lü, Y., Ciais, P., Feng, X., and Wang, Y.: Reduced sediment
- transport in the Yellow River due to anthropogenic changes, Nature Geosci, 9, 38-41,
- 891 https://doi.org/10.1038/ngeo2602, 2016.





- 892 Wang, S., Song, S., Zhang, H., Yu, L., Jiao, C., Li, C., Wu, X., Zhao, W., Best, J.,
- 893 Roberts, P., and Fu, B.: Anthropogenic impacts on the Yellow River Basin, Nat Rev
- 894 Earth Environ, 6, 656–671, https://doi.org/10.1038/s43017-025-00718-2, 2025.
- 895 Wang, T., Teng, F., and Zhang, X.: Assessing global and national economic losses from
- 896 climate change: a study based on CGEM-IAM in China, Clim. Change Econ., 11,
- 897 2041003, https://doi.org/10.1142/S2010007820410031, 2020b.
- 898 Wang, Y., Zhao, W., Wang, S., Feng, X., and Liu, Y.: Yellow River water rebalanced by
- 899 human regulation, Sci Rep, 9, 9707, https://doi.org/10.1038/s41598-019-46063-5, 2019.
- 900 Wei, Z., Jian, Z., Sun, Y., Pan, F., Han, H., Liu, Q., and Mei, Y.: Ecological sustainability
- 901 and high-quality development of the Yellow River Delta in China based on the
- 902 improved ecological footprint model, Sci Rep, 13, 3821,
- 903 https://doi.org/10.1038/s41598-023-30896-2, 2023.
- 904 Wu, J. and Gao, X.: Agridded daily observation dataset over China region and
- comparison with the other datasets, Chinese Journal of Geophysics, 56, 1102–1111,
- 906 https://doi.org/10.6038/cjg20130406, 2013.
- 907 Wu, X., Yan, Z., Yang, H., Wang, S., Zhang, H., Shen, Y., Song, S., Liu, Y., Guo, Y.,
- 908 Yang, D., and Fu, B.: Ecological restoration in the Yellow River Basin enhances
- 909 hydropower potential, Nat Commun, 16, 2566, https://doi.org/10.1038/s41467-025-
- 910 57891-7, 2025.
- 911 Wu, Z., Li, Y., Wang, R., Xu, X., Ren, D., Huang, Q., Xiong, Y., and Huang, G.:
- 912 Evaluation of irrigation water saving and salinity control practices of maize and
- 913 sunflower in the upper Yellow River basin with an agro-hydrological model based
- 914 method, Agricultural Water Management, 278, 108157,
- 915 https://doi.org/10.1016/j.agwat.2023.108157, 2023.
- 916 Xu, S., Wang, R., Gasser, T., Ciais, P., Peñuelas, J., Balkanski, Y., Boucher, O., Janssens,
- 917 I. A., Sardans, J., Clark, J. H., Cao, J., Xing, X., Chen, J., Wang, L., Tang, X., and Zhang,
- 918 R.: Delayed use of bioenergy crops might threaten climate and food security, Nature,
- 919 609, 299–306, https://doi.org/10.1038/s41586-022-05055-8, 2022.
- 920 Xu, W., Xiao, Y., Zhang, J., Yang, W., Zhang, L., Hull, V., Wang, Z., Zheng, H., Liu, J.,
- 921 Polasky, S., Jiang, L., Xiao, Y., Shi, X., Rao, E., Lu, F., Wang, X., Daily, G. C., and
- 922 Ouyang, Z.: Strengthening protected areas for biodiversity and ecosystem services in
- 923 China, Proc. Natl. Acad. Sci. U.S.A., 114, 1601–1606,
- 924 https://doi.org/10.1073/pnas.1620503114, 2017.
- 925 Xu, X., Liu, J., Zhang, S., Li, R., Yan, C., and Wu, S.: China land use remote sensing
- 926 monitoring dataset, https://doi.org/10.12078/2018070201, 2018.





- 927 Yan, Z., Wang, T., Ma, T., and Yang, D.: Water-carbon-sediment synergies and trade-
- 928 offs: Multi-faceted impacts of large-scale ecological restoration in the Middle Yellow
- 929 River Basin, Journal of Hydrology, 634, 131099,
- 930 https://doi.org/10.1016/j.jhydrol.2024.131099, 2024.
- 931 Yang, D., Shao, W., Yeh, P. J.-F., Yang, H., Kanae, S., and Oki, T.: Impact of vegetation
- 932 coverage on regional water balance in the nonhumid regions of China, Water Resources
- 933 Research, 45, https://doi.org/10.1029/2008WR006948, 2009.
- 934 Yang, Z., Li, Q., Xue, W., and Xu, Z.: Impacts of nature reserves on local residents'
- 935 income in China, Ecological Economics, 199, 107494,
- 936 https://doi.org/10.1016/j.ecolecon.2022.107494, 2022.
- 937 Ye, Q., Liu, Q., Swamy, D., Gao, L., Moallemi, E. A., Rydzak, F., and Eker, S.: FeliX
- 938 2.0: An integrated model of climate, economy, environment, and society interactions,
- 939 Environmental Modelling & Software, 179, 106121,
- 940 https://doi.org/10.1016/j.envsoft.2024.106121, 2024.
- 941 Yin, P., Gao, Y., Chen, R., Liu, W., He, C., Hao, J., Zhou, M., and Kan, H.: Temperature-
- 942 related death burden of various neurodegenerative diseases under climate warming: a
- 943 nationwide modelling study, Nat Commun, 14, 8236, https://doi.org/10.1038/s41467-
- 944 023-44066-5, 2023a.
- 945 Yin, S., Gao, G., Ran, L., Lu, X., and Fu, B.: Spatiotemporal Variations of Sediment
- 946 Discharge and In-Reach Sediment Budget in the Yellow River From the Headwater to
- 947 the Delta, Water Resources Research, 57, e2021WR030130,
- 948 https://doi.org/10.1029/2021WR030130, 2021.
- 949 Yin, S., Gao, G., Ran, L., Li, D., Lu, X., and Fu, B.: Extreme streamflow and sediment
- 950 load changes in the Yellow River Basin: Impacts of climate change and human activities,
- 951 Journal of Hydrology, 619, 129372, https://doi.org/10.1016/j.jhydrol.2023.129372,
- 952 2023b.
- 953 Yoon, J., Klassert, C., Selby, P., Lachaut, T., Knox, S., Avisse, N., Harou, J., Tilmant,
- 954 A., Klauer, B., Mustafa, D., Sigel, K., Talozi, S., Gawel, E., Medellín-Azuara, J.,
- 955 Bataineh, B., Zhang, H., and Gorelick, S. M.: A coupled human-natural system analysis
- 956 of freshwater security under climate and population change, Proceedings of the
- 957 National Academy of Sciences, 118, e2020431118,
- 958 https://doi.org/10.1073/pnas.2020431118, 2021.
- 959 YRCCMWR: Yellow River Basin Comprehensive Planning (2012-2030), 2015.
- 960 YRCCMWR: Yellow River Water Resources Bulletin, 2020.
- 961 Yu, T., Sun, R., Xiao, Z., Zhang, Q., Liu, G., Cui, T., and Wang, J.: Estimation of Global





- 962 Vegetation Productivity from Global LAnd Surface Satellite Data, Remote Sensing, 10,
- 963 327, https://doi.org/10.3390/rs10020327, 2018.
- 964 Zhang, H., Li, R., Cai, X., Zheng, C., Liu, L., Liu, M., Zhang, Q., Lin, H., Chen, L.,
- 965 and Wang, X.: Do electricity flows hamper regional economic-environmental equity?,
- 966 Applied Energy, 326, 120001, https://doi.org/10.1016/j.apenergy.2022.120001, 2022a.
- 967 Zhang, Q., Gu, X., Singh, V. P., Kong, D., and Chen, X.: Spatiotemporal behavior of
- 968 floods and droughts and their impacts on agriculture in China, Global and Planetary
- 969 Change, 131, 63–72, https://doi.org/10.1016/j.gloplacha.2015.05.007, 2015.
- 270 Zhang, T., Su, X., Zhang, G., Wu, H., and Liu, Y.: Projections of the characteristics and
- 971 probability of spatially concurrent hydrological drought in a cascade reservoirs area
- 972 under CMIP6, Journal of Hydrology, 613, 128472,
- 973 https://doi.org/10.1016/j.jhydrol.2022.128472, 2022b.
- 274 Zhou, F., Bo, Y., Ciais, P., Dumas, P., Tang, Q., Wang, X., Liu, J., Zheng, C., Polcher,
- 975 J., Yin, Z., Guimberteau, M., Peng, S., Ottle, C., Zhao, X., Zhao, J., Tan, Q., Chen, L.,
- 976 Shen, H., Yang, H., Piao, S., Wang, H., and Wada, Y.: Deceleration of China's human
- 977 water use and its key drivers, Proceedings of the National Academy of Sciences, 117,
- 978 7702–7711, https://doi.org/10.1073/pnas.1909902117, 2020.
- 979 Zhu, Y., Jia, X., Qiao, J., and Shao, M.: What is the mass of loess in the Loess Plateau
- 980 of China?, Science Bulletin, 64, 534–539, https://doi.org/10.1016/j.scib.2019.03.021,
- 981 2019.